The Complexation of the Diquat Dication by Dibenzo-3*n*-crown-*n* Ethers

Howard M. Colquhoun and Eric P. Goodings
New Science Group, Imperial Chemical Industries PLC, The Heath, Runcorn WA7 4QE
**John M. Maud,† J. Fraser Stoddart,* and John B. Wolstenholme**
Department of Chemistry, The University, Sheffield S3 7HF
David J. Williams
Chemical Crystallography Laboratory, Department of Chemistry, Imperial College, London SW7 2AY

Spectrophotometric investigations of equimolar mixtures of diquat bis(hexafluorophosphate) (2) and a range of dibenzo-3*n*-crown-*n* ethers [*n* = 6—12; (10)—(16)] in acetonitrile reveal the existence of charge-transfer absorption bands at *ca*. $\lambda_{max.}$ 400 nm. These absorptions are attributable to intermolecular π–π charge transfer between the electron-rich catechol units of the dibenzo-crown ethers and the electron-deficient bipyridinium ring system of the diquat dication. The qualitative conclusion from these experiments, that the most stable 1:1 complex is formed between dibenzo-30-crown-10 (**14**) and diquat bis(hexafluorophosphate) (**2**), led to the isolation from dichloromethane methanol—n-heptane of red crystals of [diquat.dibenzo-30-crown-10][PF$_6$]$_2$ suitable for X-ray crystallography. Although the crystal structure analysis revealed that there are two independent sets of 1:1 complexes (I and II) in the unit cell, the gross structural features of the two complexes are very similar. In addition to the parallel alignment of their three aromatic rings to accommodate the stabilising intermolecular π–π charge-transfer interaction, there is probably some further host–guest stabilisation to be gained on account of favourable electrostatic interactions between the phenolic oxygen atoms in the host and the nitrogen atoms in the pyridinium rings of the guest. Moreover, there is some evidence for weak C–H ⋯ O hydrogen bonding involving principally H-6 and H-6′ on the bipyridinium ring system of the guest and certain –CH$_2$OCH$_2$– oxygen atoms in the host. As evidenced by ^{1}H n.m.r. spectroscopy in CD$_3$COCD$_3$, these non-covalent bonding interactions are probably responsible for the formation of stable and ordered 1:1 complexes with similar gross structural features in solution, at least in the cases where dibenzo-30-crown-10 (**14**), dibenzo-33-crown-11 (**15**), and dibenzo-36-crown-12 (**16**) are the hosts. Further evidence for the 1:1 stoicheiometry of these solution complexes, as well as for the complex involving dibenzo-27-crown-9 (**13**), has come from equilibrium constant measurements for the association between the dibenzo-3*n*-crown-*n* (*n* = 9—12) hosts (**13**)—(**16**) and diquat bis(hexafluorophosphate) (**2**) in acetone. A quantitative treatment of the charge-transfer absorption bands at 400 nm, which affords K_a values of 410, 17 500, 10 800, and 2 000 M^{-1} for *n* = 9, 10, 11, and 12, respectively, provides convincing quantitative evidence for (*a*) 1:1 stoicheiometry and (*b*) the relative stabilities of the 1:1 complexes in solution. In the case of dibenzo-24-crown-8 (**12**), a complex of 2:1 (guest:host) stoicheiometry is believed to be formed in acetone with a K_a value of 385 000 M^{-2}, as shown by a successful quantitative treatment of the charge-transfer absorption data by an independent method.

Previously, we have shown [1,2] that the 2,2′-bipyridyl complex, [Pt(bipy)(NH$_3$)$_2$][PF$_6$]$_2$ (**1**), forms stable adducts in solution with dibenzo-3*n*-crown-*n* ethers [3] where *n* = 6—12. Moreover, 1:1 crystalline adducts have been isolated in the cases where dibenzo-24-crown-8,[2] dibenzo-30-crown-10,[1,2] and dibenzo-33-crown-11[2] are the hosts. The X-ray crystal structure of the 1:1 adduct formed between (**1**) and dibenzo-30-crown-10 reveals [1,2] almost complete encapsulation by the host of the dicationic guest. In addition to the expected N–H ⋯ O hydrogen-bond formation between the *cis*-ammine ligands on platinum and the polyether chains of the crown, the benzene rings (π-donors) in dibenzo-30-crown-10 enter into stabilising charge-transfer interactions with the aromatic rings of the 2,2′-bipyridyl ligand in the transition metal complex. These observations prompted us to question whether organic bipyridinium dications would also behave as guest species towards dibenzo-3*n*-crown-*n* ethers. The first and most obvious guest species to examine as a candidate for this kind of complexation is the well known

(1)

(2)
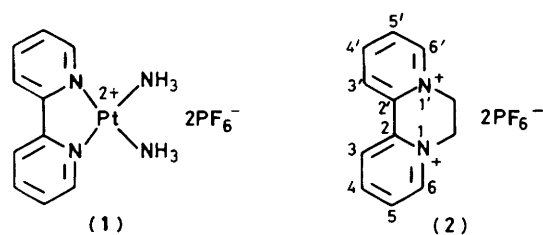
bipyridinium herbicide,[4] diquat.‡ Diquat is structurally similar to [Pt(bipy)(NH$_3$)$_2$]$^{2+}$ in so far as (*i*) it is a dication and (*ii*) it contains a 2,2′-bipyridyl residue. This paper describes the complexation in both the solution and solid states of the diquat dication, as its bis(hexafluorophosphate) salt (**2**), by a range of dibenzo-3*n*-crown-*n* ethers (*n* = 6—12) and related hosts. Recently, our preliminary results have been summarised in a communication.[5]
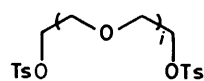
‡ The systematic name for diquat is 6,7-dihydrodipyrido[1,2-*a*:2′,1′-*c*]pyrazidinium.
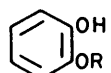
Results and Discussion

Synthesis of Crown Ether Hosts.—It will be convenient in this paper to employ the widely accepted notation of letters and numbers to identify the different crown ether hosts. Thus, the first number (3n) in the general descriptor 3nCn represents the size of the macrocyclic ring, the letter, C, the crown ether constitution of repeating unit –OCCO–, and the second number, n, the number of oxygen atoms in the ring. The letters, B, DB, and DN preceding this description stand for fused benzo-, dibenzo-, and di-(2,3)-naphtho rings, respectively. We believe this trivial system of identifiers aids both understanding and assimilation of data.
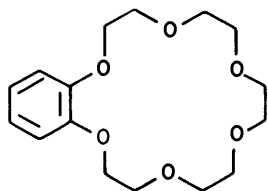
B18C6[3] (9) was isolated from the reaction (NaH, THF) between catechol (7) and pentaethyleneglycol bistosylate[6] (6). Of the range of dibenzo-crown ethers required as hosts, DB18C6[3] (10) and DB24C8[3] (11) were obtained commercially. DB21C7[3] (12), DB27C9[7] (13), DB30C10[3] (14), DB33C11 (15), and DB36C12 (16) were prepared in a stepwise manner from the monobenzyl ether[8] (8) of catechol (7) and the appropriate bistosylates[6] [(3), (4), (5), or (6)] of di-, tri-, tetra-, or pentaethyleneglycol by the procedure outlined in Scheme 1. It involves (i) the base-promoted syntheses of the acyclic polyethers [(17), (18), or (19)] and then (ii) catalytic hydrogenolysis of the benzyl ether protecting groups to afford the diphenols (20), (21), and (22), respectively followed by (iii) base-promoted macrocycle formation. DN30C10 (27) was prepared by an analogous route [i.e. (23)→(24)→(25)→(26)→(27)] from 2,3-dihydroxynaphthalene (23). The 28-membered ring compound[3] (30), incorporating two benzo-rings in the form of catechol units, but otherwise lacking the crown ether repeating unit, –OCH₂CH₂O–, was also synthesised in a stepwise manner [i.e., (8)→(28)→(29)→(30)] from the monobenzyl ether (8) of catechol (7) employing 1,10-dibromodecane as the source of the two decamethylene chains in the model macrocycle (30).
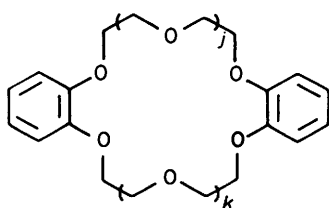
Qualitative Spectrophotometric Investigations.—The u.v. absorption spectrum of the diquat dication in water has been interpreted previously[9,10] in terms of the nearly coplanar conformation of the bipyridinium ring system. Significantly, however, there is also a much weaker absorption (ε ca. 20 l mol⁻¹ cm⁻¹) maximum at ca. 425 nm in the visible region of the electronic spectrum of a solution of diquat bis(hexafluorophosphate) (2) recorded in acetonitrile. The origin of this transition is uncertain. It may arise from an electronic transition characteristic solely of the diquat dication. Alternatively, it may be caused by a charge-transfer transition involving the diquat dication as electron acceptor and either (i) the hexafluorophosphate anion or (ii) the solvent, acetonitrile, as electron donor. The absorption is enhanced in the presence of 1 molar equivalent of either B18C6 (9) or DB18C6 (10). There is a concomitant, but small, movement of the absorption maximum to lower wavelength. DB24C8 (11) produces a somewhat greater enhancement, and a 1:1 equimolar mixture of diquat bis(hexafluorophosphate) (2) and DB30C10 (14) has, at the same molar concentration (3 × 10⁻³M), an absorbance some 20 times greater than that of diquat bis(hexafluorophosphate) (2) alone. The effect is markedly less for 1:1 equimolar mixtures of diquat bis(hexafluorophosphate) (2) with either (i) DB36C12 (16) or (ii) DN30C10 (27). These results are summarised in Figure 1.

$$2 \begin{array}{c}\text{OH} \\ \text{OCH}_2\text{Ph}\end{array} \xrightarrow[\text{NaH,THF}]{(i = 2, 3, \text{or } 4)}$$

(8)

(17) $j = 2$
(18) $j = 3$
(19) $j = 4$

Pd–C | H₂

(20) $j = 2$
(21) $j = 3$
(22) $j = 4$

NaH, THF

($i = 1, 2, 3,$ or 4)

(12) $j = 2$; $k = 1$ (DB21C7)
(13) $j = 3$; $k = 2$ (DB27C9)
(14) $j = k = 3$ (DB30C10)
(15) $j = 4$; $k = 3$ (DB33C11)
(16) $j = k = 4$ (DB36C12)

Scheme 1.

(3) $i = 1$
(4) $i = 2$
(5) $i = 3$
(6) $i = 4$

(7) R = H
(8) R = CH₂Ph

(9) (B18C6)

(10) $j = k = 1$ (DB18C6)
(11) $j = k = 2$ (DB24C8)

(23) R = H
(24) R = CH₂Ph

(25) R = CH₂Ph
(26) R = H

(27) (DN30C10)

(28) R = CH₂Ph
(29) R = H

(30)

Figure 1. The charge-transfer absorption bands (3 × 10⁻³M; 1 cm cell) in acetonitrile of diquat bis(hexafluorophosphate) (2) and its 1:1 complexes with selected crown ethers. A, [Diquat]²⁺.DB30C10; B, [diquat]²⁺.DN30C10; C, [diquat]²⁺.DB36C12; D, [diquat]²⁺. DB24C8; E, [diquat]²⁺.DB18C6; F, [diquat]²⁺.B18C6; and G, [diquat]²⁺
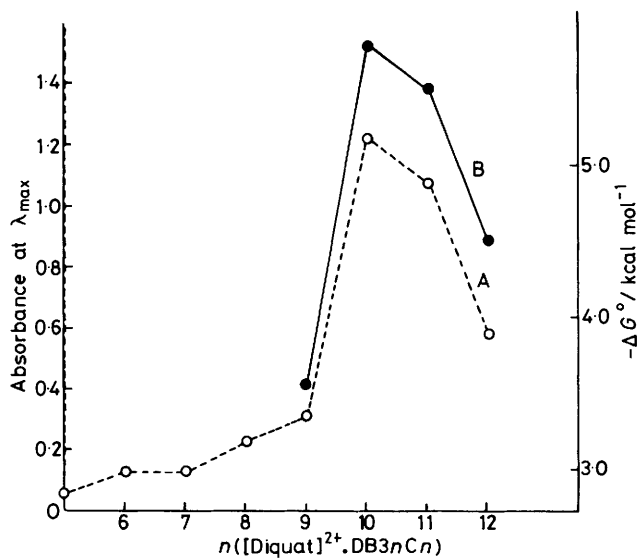
Figure 2. The dependence of the charge-transfer absorption intensities in the visible spectra of equimolar amounts (3 × 10⁻³M; 1 cm cell) of diquat bis(hexafluorophosphate) (2) and the dibenzo-crown ethers in acetonitrile upon the ring size of the macrocyclic hosts. Superimposed upon this plot (A) is a plot (B) of −Δ$G°$ versus n for the 1:1 complexes formed between diquat bis(hexafluorophosphate) (2) and the dibenzo-3n-crown-n ethers (n = 9—12) in acetone

The dependences of the absorbances at $\lambda_{max.}$ for the full range of dibenzo-crown ethers investigated, including the constitutionally asymmetric representatives, DB21C7 (12), DB27C9 (13), and DB33C11 (15), are highlighted in Figure 2. We believe these absorptions, which occur at ca. 400 nm in the 1:1 equimolar mixtures with dibenzo-crown ethers, are attributable to intermolecular charge transfer between the diquat dication as electron acceptor and the catechol moieties of the benzo-crown ethers as electron donors. The diquat dication has been shown[4] previously to form charge-transfer complexes with electron-donor anions such as iodide and ferrocyanide,[11] and with the 7,7,8,8-tetracyanoquinodimethane radical anion.[12] In addition, the related paraquat dication is known[4] to form intermolecular charge-transfer complexes with a wide range of neutral π-electron-donating organic molecules,[13] including 2-naphthol, 4,4'-dihydroxybiphenyl, hydroquinone, and catechol.

Intuitively, on the basis of the information portrayed in Figure 2, one feels that the association constant for complexation in solution between the diquat dication and a dibenzo-crown ether should be optimal when the host is DB30C10 (14). However, the observed absorbance will depend inter alia upon (i) the stoicheiometry of the complex, (ii) the association constant for complexation, and (iii) the molar

absorptivity of the complex. The qualitative studies which have been described in this section shed no light on these factors. The quantitative investigations which are described later in this paper demonstrate how these factors can be measured and understood.

Preparation of a Crystalline Complex.—Diquat bis(hexafluorophosphate) (2) and dibenzo-crown ethers dissolve separately in organic solvents such as acetonitrile and acetone

Table 1. Fractional co-ordinates of the non-hydrogen atoms ($\times 10^4$) with e.s.d.s in parentheses

Atom	x	y	z
C(1)	1 753(14)	3 659(6)	2 313(5)
C(2)	2 255(13)	3 923(7)	2 619(5)
C(3)	3 899(16)	3 997(10)	3 022(4)
C(4)	4 923(21)	3 805(13)	3 147(6)
C(5)	6 678(18)	4 299(7)	2 919(4)
C(6)	7 749(15)	4 147(8)	2 718(4)
C(7)	8 336(11)	3 859(7)	2 141(4)
C(8)	7 892(12)	3 728(6)	1 771(4)
C(9)	6 945(11)	2 935(7)	1 465(4)
C(10)	6 865(14)	3 279(7)	1 153(5)
C(11)	6 376(16)	3 019(9)	840(5)
C(12)	6 003(17)	2 434(8)	817(5)
C(13)	6 074(15)	2 088(6)	1 128(4)
C(14)	6 570(12)	2 326(6)	1 445(4)
C(15)	6 595(15)	1 407(6)	1 719(4)
C(16)	6 869(15)	1 098(7)	2 036(5)
C(17)	6 513(17)	911(10)	2 635(5)
C(18)	5 812(18)	723(12)	2 832(6)
C(19)	4 082(20)	754(11)	3 147(5)
C(20)	2 905(17)	723(9)	3 144(5)
C(21)	1 118(13)	1 108(7)	2 870(5)
C(22)	600(13)	1 306(6)	2 516(4)
C(23)	716(12)	2 135(6)	2 122(4)
C(24)	163(13)	1 822(8)	1 862(5)
C(25)	−81(14)	2 096(8)	1 533(4)
C(26)	236(15)	2 673(10)	1 476(5)
C(27)	794(14)	3 011(8)	1 738(6)
C(28)	1 014(14)	2 753(6)	2 084(5)
O(1)	1 523(9)	3 027(4)	2 370(3)
O(2)	3 407(8)	3 691(4)	2 723(2)
O(3)	5 904(9)	3 798(5)	2 908(3)
O(4)	7 379(7)	4 004(4)	2 358(2)
O(5)	7 350(8)	3 139(4)	1 780(2)
O(6)	6 689(8)	2 024(3)	1 757(2)
O(7)	6 148(8)	1 216(4)	2 315(2)
O(8)	4 650(10)	794(7)	2 859(3)
O(9)	2 351(9)	1 060(5)	2 869(2)
O(10)	1 004(7)	1 905(4)	2 457(2)
C(29)	4 971(12)	3 648(6)	2 030(4)
C(30)	4 628(12)	3 996(7)	1 742(4)
C(31)	3 970(15)	3 784(8)	1 456(4)
C(32)	3 622(11)	3 182(7)	1 468(4)
C(33)	3 927(11)	2 834(6)	1 756(4)
C(34)	3 589(10)	2 197(5)	1 774(4)
C(35)	3 182(13)	1 896(6)	1 475(4)
C(36)	2 806(13)	1 316(8)	1 514(4)
C(37)	2 903(13)	1 018(7)	1 829(5)
C(38)	3 344(13)	1 319(7)	2 111(4)
C(39)	4 071(12)	2 252(6)	2 419(3)
C(40)	5 071(11)	2 678(6)	2 319(3)
N(1)	4 624(8)	3 068(4)	2 025(3)
N(2)	3 679(9)	1 912(4)	2 092(2)
C(41)	12 010(14)	996(5)	9 444(5)
C(42)	12 043(14)	714(7)	9 804(4)
C(43)	10 938(14)	640(7)	10 307(4)
C(44)	10 057(14)	918(8)	10 528(4)
C(45)	7 922(17)	1 079(6)	10 546(4)
C(46)	6 774(14)	1 004(8)	10 342(4)
C(47)	5 638(11)	1 453(6)	9 895(4)
C(48)	5 682(14)	1 666(5)	9 528(4)
C(49)	6 431(12)	2 515(8)	9 218(4)
C(50)	6 186(13)	2 229(8)	8 899(5)
C(51)	6 463(18)	2 537(11)	8 588(5)
C(52)	6 857(19)	3 101(13)	8 614(7)
C(53)	7 149(14)	3 391(10)	8 916(7)
C(54)	6 933(12)	3 088(8)	9 233(6)
C(55)	7 566(14)	3 909(6)	9 601(5)
C(56)	7 755(18)	4 077(8)	9 944(5)
C(57)	9 080(24)	3 922(21)	10 425(8)
C(58)	10 007(22)	3 972(16)	10 561(7)

Table 1. (*continued*)

Atom	x	y	z
C(59)	12 044(16)	4 094(8)	10 511(5)
C(60)	13 056(16)	3 960(8)	10 335(5)
C(61)	14 122(11)	3 322(6)	9 992(4)
C(62)	13 918(11)	3 238(5)	9 612(4)
C(63)	13 040(12)	2 522(6)	9 230(4)
C(64)	13 190(13)	2 859(7)	8 939(4)
C(65)	12 839(15)	2 664(8)	8 591(5)
C(66)	12 311(15)	2 116(9)	8 539(5)
C(67)	12 157(13)	1 750(7)	8 826(5)
C(68)	12 509(13)	1 947(7)	9 172(5)
O(11)	12 377(8)	1 630(4)	9 479(3)
O(12)	11 071(7)	957(4)	9 989(2)
O(13)	8 918(8)	878(4)	10 345(2)
O(14)	6 796(8)	1 402(4)	10 057(2)
O(15)	6 278(8)	2 245(4)	9 535(2)
O(16)	7 180(8)	3 306(4)	9 568(3)
O(17)	8 778(9)	3 758(5)	10 090(3)
O(18)	11 055(10)	3 856(8)	10 400(4)
O(19)	13 123(9)	3 457(4)	10 172(3)
O(20)	13 251(7)	2 680(3)	9 562(2)
C(69)	8 667(12)	1 286(6)	9 480(4)
C(70)	8 509(13)	986(7)	9 179(6)
C(71)	8 759(13)	1 263(8)	8 857(4)
C(72)	9 243(11)	1 834(7)	8 864(4)
C(73)	9 411(10)	2 116(5)	9 181(3)
C(74)	9 934(10)	2 735(6)	9 205(3)
C(75)	10 025(13)	3 077(6)	8 907(4)
C(76)	10 517(13)	3 644(7)	8 936(4)
C(77)	10 898(11)	3 843(6)	9 263(5)
C(78)	10 842(12)	3 471(7)	9 565(4)
C(79)	10 343(13)	2 531(6)	9 830(3)
C(80)	9 231(12)	2 186(6)	9 819(3)
N(3)	9 126(9)	1 864(4)	9 486(3)
N(4)	10 336(9)	2 923(5)	9 519(3)
C(81)	395(15)	7 623(9)	2 002(5)
C(82)	2 406(18)	2 495(7)	688(4)
C(83)	2 715(19)	2 041(10)	509(5)
C(84)	1 414(24)	7 460(10)	2 174(8)
P(1)	9 503(3)	9 978(1)	1 596(1)
F(11)	9 757(3)	9 303(1)	1 722(1)
F(12)	9 248(3)	10 653(1)	1 471(1)
F(13)	9 485(3)	9 767(1)	1 191(1)
F(14)	9 520(3)	10 189(1)	2 001(1)
F(15)	8 121(3)	9 856(1)	1 603(1)
F(16)	10 884(3)	10 100(1)	1 590(1)
P(2)	4 468(3)	86(1)	957(1)
F(21)	4 865(3)	236(1)	1 359(1)
F(22)	4 445(3)	−613(1)	1 051(1)
F(23)	4 492(3)	786(1)	863(1)
F(24)	5 816(3)	30(1)	862(1)
F(25)	4 072(3)	−63(1)	555(1)
F(26)	3 121(3)	143(1)	1 052(1)
P(3)	1 218(3)	5 018(1)	1 535(1)
F(31)	1 313(3)	4 829(1)	1 944(1)
F(32)	1 230(3)	4 326(1)	1 423(1)
F(33)	1 206(3)	5 710(1)	1 647(1)
F(34)	1 123(3)	5 208(1)	1 126(1)
F(35)	−183(3)	4 999(1)	1 540(1)
F(36)	2 620(3)	5 037(1)	1 529(1)
P(4)	5 947(4)	5 046(1)	807(1)
F(41)	6 808(4)	4 771(1)	1 113(1)
F(42)	5 844(4)	4 400(1)	623(1)
F(43)	6 051(4)	5 691(1)	991(1)
F(44)	5 087(4)	5 320(1)	501(1)
F(45)	7 052(4)	5 199(1)	579(1)
F(46)	4 842(4)	4 893(1)	1 036(1)

giving solutions which are colourless in the concentration range 0.001—0.01M. On mixing solutions of the same solvent, a yellowish orange colour is obtained. More dramatically, diquat bis(hexafluorophosphate) (2), which is only sparingly soluble in dichloromethane, can be solubilised in this solvent by the

Table 2. Bond lengths (Å). The PF_6^- groups were treated as idealised rigid bodies with a P–F distance of 1.595 Å

Bond	Length	Bond	Length
C(1)–C(2)	1.389(24)	C(1)–O(1)	1.447(16)
C(2)–O(2)	1.444(17)	C(3)–C(4)	1.307(30)
C(3)–O(2)	1.407(20)	C(4)–O(3)	1.468(27)
C(5)–C(6)	1.504(25)	C(5)–O(3)	1.418(21)
C(6)–O(4)	1.434(18)	C(7)–C(8)	1.484(20)
C(7)–O(4)	1.431(17)	C(8)–O(5)	1.448(15)
C(9)–C(10)	1.400(22)	C(9)–C(14)	1.418(19)
C(9)–O(5)	1.331(16)	C(10)–C(11)	1.403(25)
C(11)–C(12)	1.369(27)	C(12)–C(13)	1.399(24)
C(13)–C(14)	1.398(20)	C(14)–O(6)	1.354(16)
C(15)–C(16)	1.399(22)	C(15)–O(6)	1.384(16)
C(16)–O(7)	1.391(20)	C(17)–C(18)	1.192(30)
C(17)–O(7)	1.425(22)	C(18)–O(8)	1.338(24)
C(19)–C(20)	1.340(29)	C(19)–O(8)	1.293(22)
C(20)–O(9)	1.403(21)	C(21)–C(22)	1.495(22)
C(21)–O(9)	1.406(18)	C(22)–O(10)	1.429(15)
C(23)–C(24)	1.334(22)	C(23)–C(28)	1.422(19)
C(23)–O(10)	1.383(17)	C(24)–C(25)	1.395(24)
C(25)–C(26)	1.351(27)	C(26)–C(27)	1.372(28)
C(27)–C(28)	1.435(29)	C(28)–O(1)	1.343(21)
C(29)–C(30)	1.374(20)	C(29)–N(1)	1.347(16)
C(30)–C(31)	1.364(21)	C(31)–C(32)	1.395(24)
C(32)–C(33)	1.363(19)	C(33)–C(34)	1.471(18)
C(33)–N(1)	1.357(16)	C(34)–C(35)	1.370(19)
C(34)–N(2)	1.354(17)	C(35)–C(36)	1.368(23)
C(36)–C(37)	1.359(24)	C(37)–C(38)	1.333(23)
C(38)–N(2)	1.373(18)	C(39)–C(40)	1.541(18)
C(39)–N(2)	1.494(15)	C(40)–N(1)	1.475(15)
C(41)–C(42)	1.494(23)	C(41)–O(11)	1.473(15)
C(42)–O(12)	1.440(18)	C(43)–C(44)	1.469(22)
C(43)–O(12)	1.406(17)	C(44)–O(13)	1.439(18)
C(45)–C(46)	1.489(24)	C(45)–O(13)	1.461(21)
C(46)–O(14)	1.392(18)	C(47)–C(48)	1.467(21)
C(47)–O(14)	1.428(15)	C(48)–O(15)	1.455(15)
C(49)–C(50)	1.375(25)	C(49)–C(54)	1.396(24)
C(49)–O(15)	1.354(19)	C(50)–C(51)	1.407(29)
C(51)–C(52)	1.332(37)	C(52)–C(53)	1.334(36)
C(53)–C(54)	1.404(32)	C(54)–O(16)	1.368(22)
C(55)–C(56)	1.352(27)	C(55)–O(16)	1.414(16)
C(56)–O(17)	1.446(22)	C(57)–C(58)	1.154(37)
C(57)–O(17)	1.340(32)	C(58)–O(18)	1.389(28)
C(59)–C(60)	1.389(26)	C(59)–O(18)	1.292(22)
C(60)–O(19)	1.277(21)	C(61)–C(62)	1.448(19)
C(61)–O(19)	1.386(16)	C(62)–O(20)	1.461(14)
C(63)–C(64)	1.347(21)	C(63)–C(68)	1.427(20)
C(63)–O(20)	1.308(15)	C(64)–C(65)	1.417(24)
C(65)–C(66)	1.367(26)	C(66)–C(67)	1.370(25)
C(67)–C(68)	1.414(25)	C(68)–O(11)	1.369(20)
C(69)–C(70)	1.322(26)	C(69)–N(3)	1.387(17)
C(70)–C(71)	1.402(27)	C(71)–C(72)	1.384(23)
C(72)–C(73)	1.352(19)	C(73)–C(74)	1.498(17)
C(73)–N(3)	1.331(16)	C(74)–C(75)	1.365(18)
C(74)–N(4)	1.313(15)	C(75)–C(76)	1.382(21)
C(76)–C(77)	1.359(23)	C(77)–C(78)	1.409(23)
C(78)–N(4)	1.354(19)	C(79)–C(80)	1.477(20)
C(79)–N(4)	1.461(16)	C(80)–N(3)	1.446(16)
C(81)–C(84)	1.348(32)	C(82)–C(83)	1.274(25)

addition of 1 molar equivalent of DB30C10 (**14**) to the extent that a 0.1M-solution displays an intense red colour. The colours are, of course, attributable to charge transfer between the electron-rich catechol units of DB30C10 (**14**) and the electron-deficient bipyridinium ring system of the diquat dication discussed in the previous section. When pentane was layered above the dichloromethane solution, dark red needles, which when analysed gave 1:1 guest–host stoicheiometry, were obtained. Single crystals of a 1:1 complex between diquat

Table 3. Bond angles (°). The PF_6^- groups were treated as idealised rigid bodies with bond angles of 90 and 180° as appropriate

Bonds	Angle	Bonds	Angle
C(2)–C(1)–O(1)	110.7(14)	C(1)–C(2)–O(2)	113.9(13)
C(4)–C(3)–O(2)	116.2(19)	C(3)–C(4)–O(3)	118.2(19)
C(6)–C(5)–O(3)	109.0(13)	C(5)–C(6)–O(4)	108.7(13)
C(8)–C(7)–O(4)	110.4(10)	C(7)–C(8)–O(5)	106.4(11)
C(10)–C(9)–C(14)	118.0(13)	C(10)–C(9)–O(5)	124.5(13)
C(14)–C(9)–O(5)	117.5(12)	C(9)–C(10)–C(11)	119.1(15)
C(10)–C(11)–C(12)	123.4(17)	C(11)–C(12)–C(13)	117.7(17)
C(12)–C(13)–C(14)	120.7(14)	C(9)–C(14)–C(13)	120.9(13)
C(9)–C(14)–O(6)	114.2(11)	C(13)–C(14)–O(6)	124.9(12)
C(16)–C(15)–O(6)	112.8(12)	C(15)–C(16)–O(7)	116.0(14)
C(18)–C(17)–O(7)	121.1(19)	C(17)–C(18)–O(8)	134.4(23)
C(20)–C(19)–O(8)	122.6(17)	C(19)–C(20)–O(9)	112.9(16)
C(22)–C(21)–O(9)	111.6(13)	C(21)–C(22)–O(10)	107.3(11)
C(24)–C(23)–C(28)	122.3(15)	C(24)–C(23)–O(10)	124.0(13)
C(28)–C(23)–O(10)	113.6(13)	C(23)–C(24)–C(25)	119.4(16)
C(24)–C(25)–C(26)	120.9(16)	C(25)–C(26)–C(27)	121.4(18)
C(26)–C(27)–C(28)	119.3(16)	C(23)–C(28)–C(27)	116.5(15)
C(23)–C(28)–O(1)	117.0(15)	C(27)–C(28)–O(1)	126.5(13)
C(1)–O(1)–C(28)	113.3(12)	C(2)–O(2)–C(3)	111.3(12)
C(4)–O(3)–C(5)	117.6(15)	C(6)–O(4)–C(7)	113.3(10)
C(8)–O(5)–C(9)	114.7(10)	C(14)–O(6)–C(15)	113.5(10)
C(16)–O(7)–C(17)	113.0(12)	C(18)–O(8)–C(19)	126.3(16)
C(20)–O(9)–C(21)	116.7(12)	C(22)–O(10)–C(23)	115.0(10)
C(30)–C(29)–N(1)	117.2(12)	C(29)–C(30)–C(31)	123.5(14)
C(30)–C(31)–C(32)	116.8(15)	C(31)–C(32)–C(33)	120.5(13)
C(32)–C(33)–C(34)	121.7(12)	C(32)–C(33)–N(1)	119.5(12)
C(34)–C(33)–N(1)	118.6(11)	C(33)–C(34)–C(35)	120.8(12)
C(33)–C(34)–N(2)	118.8(11)	C(35)–C(34)–N(2)	120.4(11)
C(34)–C(35)–C(36)	117.8(13)	C(35)–C(36)–C(37)	122.7(15)
C(36)–C(37)–C(38)	117.5(15)	C(37)–C(38)–N(2)	122.4(14)
C(40)–C(39)–N(2)	107.6(9)	C(39)–C(40)–N(1)	108.3(9)
C(29)–N(1)–C(33)	122.4(11)	C(29)–N(1)–C(40)	117.5(10)
C(33)–N(1)–C(40)	120.0(10)	C(34)–N(2)–C(38)	119.0(11)
C(34)–N(2)–C(39)	120.0(10)	C(38)–N(2)–C(39)	120.9(10)
C(42)–C(41)–O(11)	108.9(12)	C(41)–C(42)–O(12)	107.3(12)
C(44)–C(43)–O(12)	112.1(12)	C(43)–C(44)–O(13)	109.1(12)
C(46)–C(45)–O(13)	112.5(12)	C(45)–C(46)–O(14)	106.1(13)
C(48)–C(47)–O(14)	110.8(11)	C(47)–C(48)–O(15)	107.7(11)
C(50)–C(49)–C(54)	121.4(17)	C(50)–C(49)–O(15)	122.5(15)
C(54)–C(49)–O(15)	116.0(15)	C(49)–C(50)–C(51)	117.3(17)
C(50)–C(51)–C(52)	119.0(20)	C(51)–C(52)–C(53)	125.8(24)
C(52)–C(53)–C(54)	116.6(20)	C(49)–C(54)–C(53)	119.4(18)
C(49)–C(54)–O(16)	115.1(16)	C(53)–C(54)–O(16)	125.5(16)
C(56)–C(55)–O(16)	112.2(15)	C(55)–C(56)–O(17)	108.4(15)
C(58)–C(57)–O(17)	129.1(28)	C(57)–C(58)–O(18)	124.9(27)
C(60)–C(59)–O(18)	119.0(16)	C(59)–C(60)–O(19)	119.2(16)
C(62)–C(61)–O(19)	114.7(10)	C(61)–C(62)–O(20)	107.0(10)
C(64)–C(63)–C(68)	116.2(14)	C(64)–C(63)–O(20)	127.3(12)
C(68)–C(63)–O(20)	116.3(13)	C(63)–C(64)–C(65)	122.8(14)
C(64)–C(65)–C(66)	120.4(16)	C(65)–C(66)–C(67)	119.3(16)
C(66)–C(67)–C(68)	120.1(15)	C(63)–C(68)–C(67)	121.2(15)
C(63)–C(68)–O(11)	113.2(14)	C(67)–C(68)–O(11)	125.7(13)
C(41)–O(11)–C(68)	117.2(12)	C(42)–O(12)–C(43)	110.0(10)
C(44)–O(13)–C(45)	115.9(11)	C(46)–O(14)–C(47)	109.2(11)
C(48)–O(15)–C(49)	117.0(11)	C(54)–O(16)–C(55)	117.6(13)
C(56)–O(17)–C(57)	112.9(19)	C(58)–O(18)–C(59)	122.3(18)
C(62)–O(20)–C(63)	114.8(10)	C(60)–O(19)–C(61)	119.6(12)
C(70)–C(69)–N(3)	121.0(15)	C(69)–C(70)–C(71)	119.8(15)
C(70)–C(71)–C(72)	118.9(15)	C(71)–C(72)–C(73)	118.8(14)
C(72)–C(73)–C(74)	121.2(11)	C(72)–C(73)–N(3)	122.4(12)
C(74)–C(73)–N(3)	116.4(10)	C(73)–C(74)–C(75)	120.4(11)
C(73)–C(74)–N(4)	117.8(11)	C(75)–C(74)–N(4)	121.8(12)
C(74)–C(75)–C(76)	119.3(13)	C(75)–C(76)–C(77)	118.5(14)
C(76)–C(77)–C(78)	121.1(14)	C(77)–C(78)–N(4)	117.4(13)
C(80)–C(79)–N(4)	108.4(10)	C(79)–C(80)–N(3)	108.3(10)
C(69)–N(3)–C(73)	119.0(11)	C(69)–N(3)–C(80)	119.0(11)
C(73)–N(3)–C(80)	121.9(10)	C(74)–N(4)–C(78)	121.8(11)
C(74)–N(4)–C(79)	121.4(11)	C(78)–N(4)–C(79)	116.6(11)

(a)

(b)

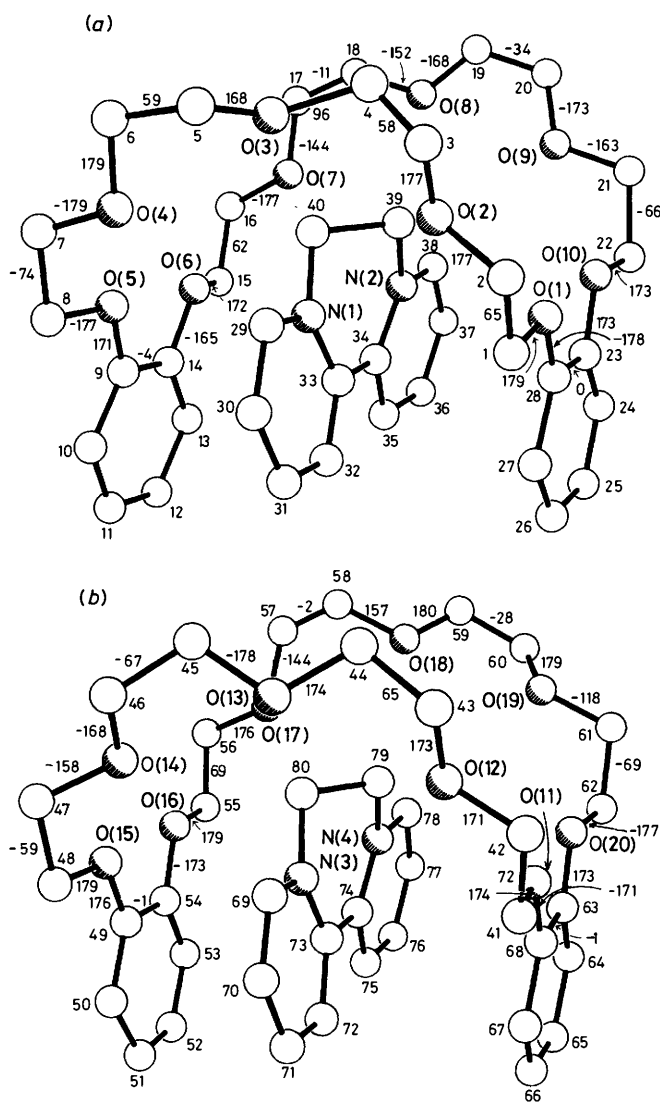**Figure 3.** The skeletal representations of the solid-state structures of the two independent complexes I (a) and II (b), found in [diquat.DB30C10]$^{2+}$. The atomic numbering scheme is shown on these framework diagrams

bis(hexafluorophosphate) (2) and DB30C10 (14), which were suitable for X-ray crystallography, were grown by the careful manipulation of three solvents, dichloromethane, methanol, and heptane.

X-*Ray Structural Investigation.*—The crystal structure analysis constituted a considerable challenge because of the fact that, in addition to general disorder in the structure, there are two independent sets of [diquat.DB30C10]$^{2+}$ complexes (I and II) in the unit cell. The atomic co-ordinates, bond lengths, and bond angles are listed for both complexes in Tables 1, 2, and 3, respectively. The torsional angles associated with the 30-membered ring in complexes I and II, respectively, are shown beside the relevant C–C and C–O bonds in the skeletal structures reproduced in Figure 3 (a and b), which also provide the details of the crystallographic numbering scheme. From an inspection of the torsional angles in Figure 3 (a and b), it is obvious that complexes I and II differ slightly in the conformations adopted by their respective polyether chains.

Table 4. Selected host–guest contact distances and relevant hydrogen contact distances and angles in order of increasing C $\cdots$ O distance

C–H $\cdots$ O^a	R(C $\cdots$ O) (Å)	R(H $\cdots$ O) (Å)	$\theta(°)^b$	$\varphi(°)^c$
C(29)–O(4)	3.05	2.19	135	13
C(29)–O(5)	3.12^d			
C(69)–O(14)	3.13	2.43	121	46
C(38)–O(9)	3.17	2.34	133	23
C(78)–O(17)	3.21^d			
C(40)–O(6)	3.22^d			
C(38)–O(7)	3.25^d			
C(78)–O(20)	3.25^d			
C(78)–O(18)	3.26	2.25	154	23
C(38)–O(10)	3.29^d			
C(38)–O(8)	3.33	2.33	153	5
C(39)–O(7)	3.33^d			
C(69)–O(12)	3.34^d			
C(40)–O(2)	3.35^d			
C(78)–O(19)	3.37^d			
C(39)–O(1)	3.37^d			
C(79)–O(11)	3.38^d			
C(69)–O(13)	3.38^d			
C(80)–O(14)	3.41^d			

^{a} The seven shortest distances, R(N $\cdots$ O) (Å), are N(1) $\cdots$ O(5), 3.28; N(2) $\cdots$ O(7), 3.28; N(1) $\cdots$ O(2), 3.33; N(4) $\cdots$ O(20), 3.35; N(3) $\cdots$ O(15), 3.36; N(2) $\cdots$ O(10), 3.40; N(4) $\cdots$ O(17), 3.40. ^{b} C–H $\cdots$ O Angles. ^{c} Angles between COC planes and HO vectors. ^{d} Either not considered to be within hydrogen-bonding distance or the geometry is inappropriate for hydrogen bonding.

The four hexafluorophosphate counterions also exhibit severe disorder. Amidst this widespread disorder, the most significant differences in the conformations of the polyether chains involve the relative dispositions of O(3) and O(13), and, to a lesser extent, those of O(8) and O(18). Disorder in the polyether chains was evidenced by large anisotropic thermal parameters. In no instance was it possible to identify discrete alternative sites for atoms displaying high thermal motion. The consequence of the disorder in the above regions of the polyether chains is reflected in an artificial shortening of some of the bonds (Table 2) and distortion of the associated angles (Table 3). This degree of disorder in the polyether chains was not evident in the crystal structure ^{1,2} of [Pt(bipy)(NH$_3$)$_2$.DB30C10][PF$_6$]$_2$ where three of the ten oxygen atoms in DB30C10 (14) participate in relatively strong N–H $\cdots$ O hydrogen bonding to three of the six hydrogen atoms in the two ammine ligands of the platinum complex. Thus, the conformational disorder in the polyether chains of [diquat.DB30C10]$^{2+}$ may reflect the relatively weak C–H $\cdots$ O hydrogen bonding, if indeed it operates as an attractive interaction in this case. The geometrical parameters for those hydrogen contacts, selected on the basis of their geometry as being amongst the most favourable for possible guest–host stabilisation, are listed in Table 4. They reveal that any C–H $\cdots$ O hydrogen bonding is more pronounced for the aromatic hydrogen atoms at C(29), C(38), C(69), and C(78) on the pyridinium rings of the guest [*i.e.*, for H(6) and H(6′), employing the bipyridinium ring numbering system illustrated in (2)] than for the hydrogen atoms at C(39), C(40), C(79), and C(80) in the bridging bismethylene unit. It is conceivable that H-6 and H-6′ are the most acidic hydrogen atoms present in the diquat dication. Attempts to exchange H(6) and H(6′) selectively for deuterium atoms by the treatment of (2) with NaOD–D$_2$O were frustrated by the high instability of the diquat dication, even in weakly basic aqueous solutions.^{4} However, it has been concluded ^{14} from base-catalysed deuterium-exchange studies on N-methylpyridinium iodide that kinetically the most acidic hydrogen atoms on the pyridinium ring are indeed those sited at
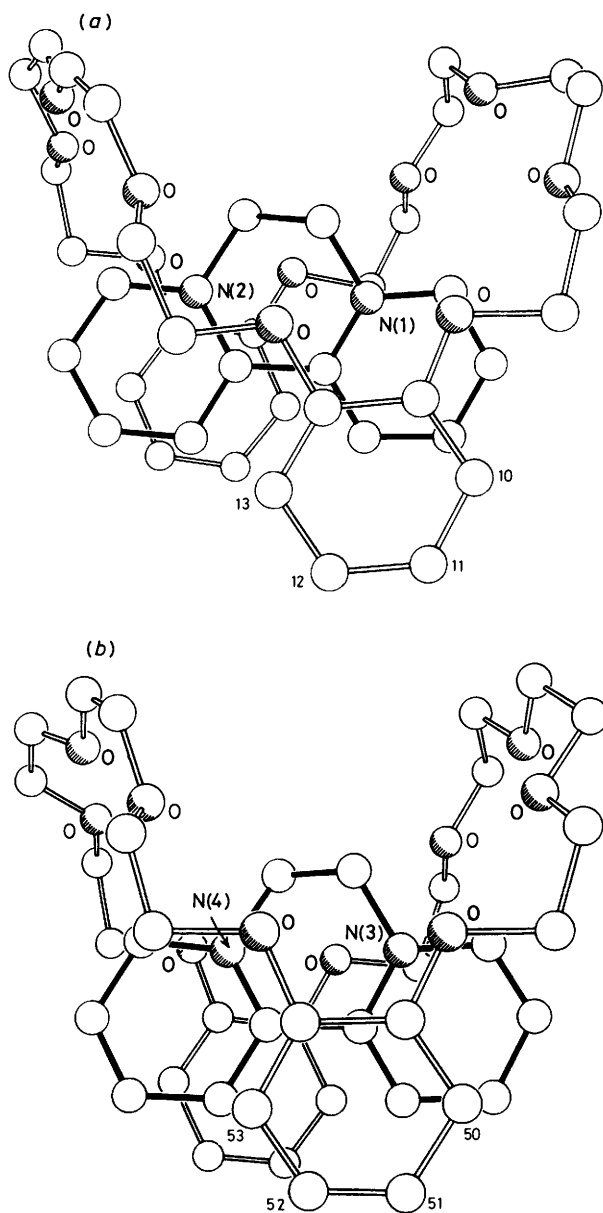
Figure 5. The space-filling representations of the solid-state structure of the 1 : 1 complex (II) formed between the diquat dication and DB30C10 (**27**)

Figure 4. Side-on views of the skeletal representations of the solid-state structures of the two independent complexes I (*a*) and II (*b*), found in [diquat.DB30C10]$^{2+}$

C(2) and C(6). The side-on views, shown in Figure 4 (*a* and *b*), of the skeletal representations of the complexes I and II, respectively, reveal that the polyether chains form hydrophilic loops around the aromatic hydrogen atoms on C(29), C(38), C(69), and C(78). The geometry of the overlap between the bipyridyl unit and the two benzo rings can clearly be seen from these side-on views. The space-filling representation of the structure of complex II, reproduced in Figure 5, also illustrates well this feature of the interaction between the diquat dication and DB30C10 (**14**). Direct visual comparison of the space-filling representation in Figure 5 with the framework representation of the structure of complex II shown in Figure 3(*b*) is necessary in order to appreciate other aspects of structural detail. In particular, the approximately parallel alignment of the two benzo-rings in DB30C10 (**14**) with the bipyridinium ring of the diquat dication is clearly displayed. The separation between the
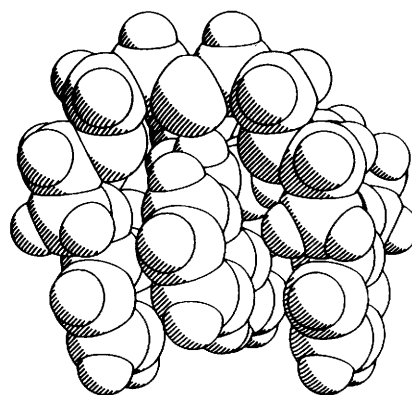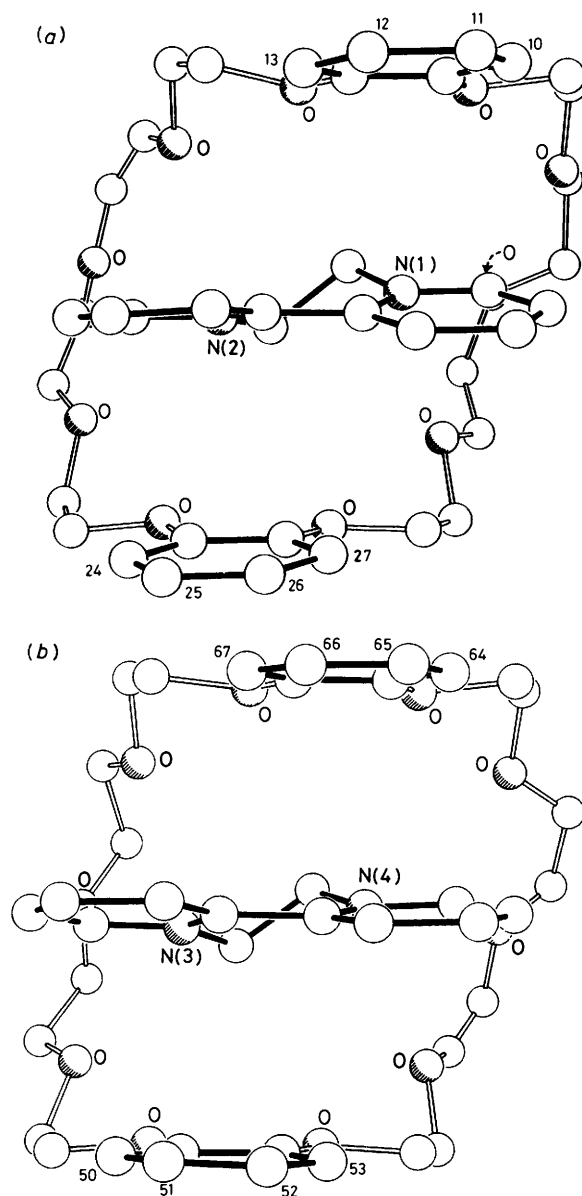
Figure 6. Underside views of the skeletal representations of the solid-state structures of the two independent complexes I (*a*) and II (*b*), found in [diquat.DB30C10]$^{2+}$

Table 5. [1]H N.m.r. chemical shift data[a] in CD_3COCD_3

| | δ Values (Δδ values) | | | | | |
	H(6), (6')[b]	H(3), (3')[b]	H(4), (4')[b]	H(5), (5')[b]	(NCH$_2$)$_2$[b]	C$_6$H$_4$[c]
(2)	9.44	9.19	9.06	8.56	5.66	
DB3nCn						6.88
(2)·DB36C12	9.33	8.63	8.55	8.37	5.68	6.88, 6.78
	(−0.11)	(−0.56)	(−0.51)	(−0.19)	(+0.02)	(0.00, −0.10)
(2)·DB33C11	9.28	8.53	8.37	8.35	5.77	6.82, 6.63
	(−0.16)	(−0.66)	(−0.69)	(−0.21)	(+0.11)	(−0.06, −0.15)
(2)·DB30C10	9.46	8.59	8.40	8.22	5.72	6.72, 6.47
	(+0.02)	(−0.60)	(−0.66)	(−0.34)	(+0.06)	(−0.16, −0.41)
(2)·DB27C9	9.48	8.84	8.84	8.43	5.75	6.82
	(+0.04)	(−0.35)	(−0.22)	(−0.13)	(+0.09)	(−0.06)
(2)·DB24C8	9.42	0.86	8.86	8.43	5.65	6.81
	(−0.02)	(−0.33)	(−0.20)	(−0.13)	(−0.01)	(−0.07)

[a] Spectra recorded at ambient temperature with a 220 MHz spectrometer and an internal reference (Me$_4$Si). [b] Guest proton signals. [c] Host aromatic proton signals.

benzo-rings in the host is 6.8 Å with only 4 and 7° departures from parallel alignments of their mean planes in complexes I and II, respectively. The average distance of 3.4 Å between the mean planes of a benzo-ring and the bipyridinium ring is ideal[15,16] for charge transfer to occur between the π-electron-rich catechol units in the host and the π-electron-deficient bipyridinium rings in the guest. The underside skeletal views of complexes I and II, shown in Figure 6 (a and b), respectively, reveal that the pyridinium rings in both cases are not quite coplanar. The dihedral angles between the mean planes of the pyridinium rings are 15 and 14°, respectively, for complexes I and II. These values may be compared with the reported[17] dihedral angles of 19.7 and 20.4° between the mean planes of the rings in crystalline diquat dibromide. In the tetracyanoquinodimethane anionic complex in the solid state,[12] the two pyridinium rings in the diquat dication exhibit a twist of 22.0° between their mean planes. In agreement with the vast majority of X-ray crystallographic data[18] on molecules with aromatic o-dimethoxy substitution, and also with their preferred conformations in solution,[19] the ortho-related oxymethylene units in the DB30C10 host (14) are nearly all coplanar [see relevant torsional angles in Figure 3 (a and b)]. This conformational feature allows delocalisation of the non-bonding electrons on the phenolic oxygen atoms into the aromatic rings by means of good overlap between the lone-pair orbitals of the phenolic oxygen atoms with the π*-orbitals of the benzo-rings. This stereoelectronic interaction probably enhances charge transfer between the π-electron-rich benzo-rings and the π-electron-deficient bipyridinium dication. Also the favourable juxtapositions [see Figure 4 (a and b)] of the phenolic oxygen atoms in the host with the nitrogen atoms in the guest probably impart some electrostatic stabilisation upon the complex. In particular, the N(1)–O(5) and N(3)–O(15) distances are 3.28 and 3.35 Å, respectively. In support of these stabilising interactions is the fact that the highly flexible DB30C10 host (14) adopts a U-shaped conformation which is markedly different from the 'flat' conformation observed[20] for the crystalline free host.

There are no significant contacts, between symmetry-related complexes, of less than normal van der Waals distances.

Although, in solution, spectroscopic evidence often reveals[21] the presence of charge-transfer complexes with 1:1 stoicheiometry as discrete pairs containing single π-donor and π-acceptor molecules, in general, in the solid state, an infinite laminate comprising alternate donor and acceptor species is often observed. By contrast, the [diquat.DB30C10]$^{2+}$ complexes constitute discrete entities in the solid state, which would

be expected to retain their gross structural features in solution, provided the intermolecular interactions are sufficiently stabilising. In this respect, the [diquat.DB30C10]$^{2+}$ complexes appear to have more in common with certain termolecular complexes[22] formed between two π-donor molecules (e.g., phenol) and one π-acceptor molecule (e.g., benzoquinone). In crystals of these 2:1 complexes, groups of three molecules are often stacked discontinuously in columns. Hence, it would be reasonable to view the solid-state structures of the [diquat.DB30C10]$^{2+}$ complexes as prototypes of the triad-like structure expected for their most stable complex in solution.

[1]*H N.m.r. Spectroscopic Investigations.*—The assignment (Table 5) of protons in the [1]H n.m.r. spectrum of diquat bis(hexafluorophosphate) (2) recorded in CD_3COCD_3 was made on the basis of comparisons with published[10,11] spectral data for diquat dibromide in D_2O. The spectral data listed in Table 5, and presented graphically in Figure 7, summarise how the chemical shifts of the (NCH$_2$)$_2$ protons and of H(3), (3'), H(4), (4'), H(5), (5'), and H(6), (6') in the diquat dication, and the aromatic protons in the hosts, are influenced by separate additions of 1 molar equivalent of the dibenzo-3n-crown-n hosts (for n = 8—12) to (2). When n = 10—12, there are (upfield) shifts of between −0.19 and −0.69 p.p.m. for H(3), (3'), H(4), (4'), and H(5), (5') on the bipyridinium ring of the guest. The aromatic protons on the benzo-rings of the host also experience (upfield) shifts of up to −0.41 p.p.m. The sign and magnitude of these shifts support a description of a 1:1 complex formed between (2) and the dibenzo-3n-crown-n ether (n = 10—12) hosts (14)—(16) in solution which is similar to that for the 1:1 complex between (2) and DB30C10 (14) in the solid state. In such a structure with parallel stacking of the aromatic rings, the considerable geometrical overlap between the aromatic rings of the host and guest presumably causes the anisotropic diamagnetic susceptibility of one aromatic system to enhance the local magnetic field experienced by ^{1}H nuclei attached to the other aromatic system. Although attempts to interpret the sign and magnitude of chemical shifts of protons in π-donors and π-acceptors involved in simple charge-transfer complexes have not been wholly successful,[23] the interpretation offered above is the most widely accepted one. Explanations based on transfer of charge in the complex or differences in the anisotropy of polar groups as a result of transfer of charge are not convincing (cf. reference 18) for at least three reasons. (i) Both the π-donors, in the form of the benzo-rings of the dibenzo-3n-crown-n ether hosts, and the π-acceptor, in the form of the bipyridinium ring of the guest, exhibit upfield shifts of their proton signals relative
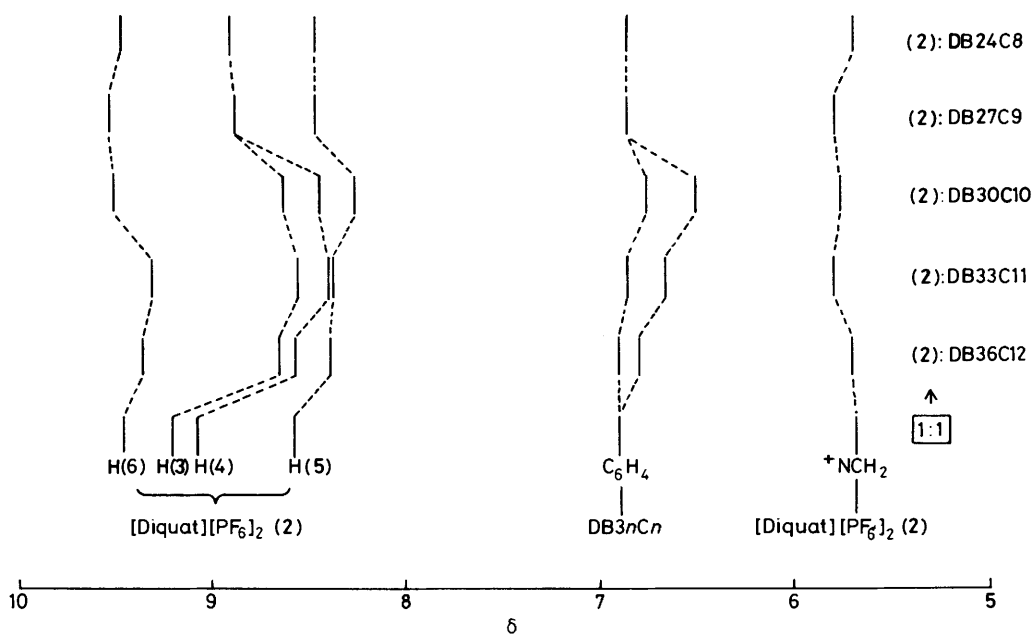
Figure 7. Partial ^{1}H n.m.r. line spectra of equimolar amounts of diquat bis(hexafluorophosphate) (2) and the dibenzo-crown ethers from DB24C8 to DB36C12 in hexadeuterioacetone compared with those of (2) and the free hosts

to those observed in the free hosts and guest. The direct effect upon chemical shifts of a transfer of charge would be expected to lead to downfield shifts of π-donor proton signals matching qualitatively the upfield shifts of the π-acceptor proton signals. (*ii*) The magnitudes of these upfield shifts are far in excess of the values that would be predicted on the basis of transfer of charge alone. (*iii*) Protons in constitutionally different positions on both the π-acceptor and π-donor aromatic rings experience markedly different upfield shifts. The signals for H(3), (3′) and H(4), (4′) are shifted upfield to a much greater extent than those for H(5), (5′), which are more distant, on average, from the anisotropic influence of the benzo-rings in the hosts [*cf*. Figure 4 (*a* and *b*)]. The chemical shift differences between the nonequivalent benzo-protons, as well as the individual magnitudes of their upfield shifts caused by complexation, reach maxima (Figure 7) when *n* = 10, *i.e.*, for DB30C10 (**14**) in the presence of 1 molar equivalent of (**2**).

The $(\overset{+}{\text{N}}\text{CH}_2)_2$ protons and H(6), (6′) in the diquat dication are believed (see the previous section) to be involved in weak C–H $\cdots$ O hydrogen bonding with oxygen atoms in the dibenzo-3*n*-crown-*n* ether hosts. Interestingly, the shifts observed on complexation are small and, in some cases, they are actually downfield. At least two factors could be contributing to the deshielding of these protons. (*i*) Intermolecular hydrogen bonding renders the hydrogen atom involved more positive and hence the proton will resonate at a lower field.[15,24] (*ii*) The diamagnetic anisotropy of the oxygen atom in ethers causes[25] a downfield shift of protons in close proximity to the local C_2 axis of a –CH$_2$OCH$_2$– fragment.

In general, the correspondence between qualitative u.v. (Figure 2) and ^{1}H n.m.r. (Figure 7) spectroscopic data is excellent. Both probes appear to suggest rather similar solution-state structures when *n* = 10, 11, and 12 for complexes between (**2**) and the hosts DB30C10 (**14**), DB33C11 (**15**), and DB36C12 (**16**), respectively. Thus, all the evidence would seem to point to solution-state structures for 1 : 1 complexes involving these hosts that are similar to those of the solid-state complexes (Figures 3—6) formed between (**2**) and DB30C10 (**14**). By the same token, the different nature of the spectra (u.v. and ^{1}H

n.m.r.) when *n* = 8 and 9 suggests that the complexes formed between (**2**) and DB24C8 (**11**), and (**2**) and DB27C9 (**13**), have solution structures different from those of the solid-state complexes formed between (**2**) and DB30C10 (**14**).

The small chemical shift changes in (OCH$_2$)$_2$ protons in the hosts on complexation are not so easy to interpret in view of their limited dispersion, even at high operating fields. Those assignments (*cf*. reference 26) made to *O*-methylene groups in the Experimental section employ a notation in which these constitutionally heterotopic groups are designated α, β, γ $\cdot\cdot\cdot$, starting adjacent to the benzo-rings and progressing along the polyether chains. In the case of the unsymmetrical dibenzo-3*n*-crown-*n* ether hosts, the larger polyether chain was designated α′, β′, γ′ $\cdot\cdot\cdot$, in like manner.

Measurement of Stability Constants.—Methods for the determination of association constants, K_a, in solution for π-donor and π-acceptor species often rely upon quantitative measurements of charge-transfer absorption bands. They have been the subject of an excellent discussion in the monograph by Foster.[27] Usually one component has been used in considerable excess over the other in these experiments. In the face of solubility problems with some of the dibenzo-crown ethers in one of the chosen solvents (acetone), and in our desire to be economical in the use of the synthetically hard-won macro-cycles, we devised an experimental procedure in which the relative concentrations of diquat bis(hexafluorophosphate) (**2**) and the dibenzo-crown ether under investigation were in-variably equimolar. Indeed, it has been suggested[16,28] that more weight should be given to K_a values obtained from optical data under these conditions than when measurements of the charge-transfer absorption band are made on solutions in which one of the solute species is present in large excess. The method that we shall now describe bears some resemblance to one utilised by Ray[29] in his investigation of intimate ion-pair formation by substituted pyridinium bromide.

Assuming that the complex formed between the diquat dication and the dibenzo-crown ethers (DBCE) has 1 : 1 stoicheiometry and that complexes with other stoicheiometries

are absent, we can define the association constant, K_a, by equation (1). If, for a solution containing equimolar amounts of

$$K_a = \frac{[\text{complex}]}{[\text{diquat}^{2+}2\text{PF}_6^-][\text{DBCE}]} \qquad (1)$$

diquat and DBCE, the total concentration of diquat is d, then it follows that the total concentration of DBCE is also d, or as given in equations (2) and (3).

$$[\text{diquat}^{2+}\,2\text{PF}_6^-] + [\text{complex}] = d \qquad (2)$$

$$[\text{DBCE}] + [\text{complex}] = d \qquad (3)$$

Letting x equal the equilibrium concentration of the complex, equation (1) becomes equation (4).

$$K_a = \frac{x}{(d - x)^2} \qquad (4)$$

In the visible spectrum recorded on the solution the measured absorbance, A, at a particular wavelength is the sum of the absorbances arising from each component, i.e., equation (5),

$$A = A_\text{D} + A_\text{CE} + A_\text{X} \qquad (5)$$

where A_D, A_CE, and A_X are the absorbances for diquat, the DBCE, and complex, respectively. Assuming that the Beer–Lambert law is obeyed for all species in solution, we get equation (6), where A_i is the absorbance arising from species i, c_i

$$A_i = c_i \varepsilon_i l \qquad (6)$$

is the molar concentration of species i, ε_i is the molar absorptivity for species i, and l is the path length of the cell. For complexation between the diquat dication and dibenzo-crown ethers it is convenient to measure A at the wavelength ($\lambda_{max.}$ is 400 nm for the diquat–DB30C10 system in acetonitrile) of maximum absorbance in the charge-transfer region. Invariably, it can be assumed that A_CE is zero at this wavelength and so equation (5) becomes equation (7), where ε_D and ε_X are the

$$A = \varepsilon_\text{D}(d - x)l + \varepsilon_\text{X}xl \qquad (7)$$

molar absorptivities of diquat and the complex, respectively. Whence we obtain equation (8). If, for convenience sake, we

$$x = \frac{A - \varepsilon_\text{D}dl}{(\varepsilon_\text{X} - \varepsilon_\text{D})l} \qquad (8)$$

identify $A - \varepsilon_\text{D}dl$ as equal to A_C and $\varepsilon_\text{X} - \varepsilon_\text{D} = \varepsilon_\text{C}$, then equation (8) can be expressed as equation (9). Combining

$$x = \frac{A_\text{C}}{\varepsilon_\text{C}l} \qquad (9)$$

equations (4) and (9), equation (10) follows.

$$\frac{d}{A_\text{C}} = \left(\frac{1}{K_a \varepsilon_\text{C}l}\right)^{\frac{1}{2}} \cdot \frac{1}{(A_\text{C})^{\frac{1}{2}}} + \frac{1}{\varepsilon_\text{C}l} \qquad (10)$$

Thus, provided 1:1 complex formation occurs and is dominant under the conditions of the experiments, a plot of d/A_C against $1/(A_\text{C})^{\frac{1}{2}}$ for a series of solutions of different concentrations d should be linear with the slope of the line equal to $(1/K_a \varepsilon_\text{C}l)^{\frac{1}{2}}$ and the intercept on the d/A_C axis equal to $1/\varepsilon_\text{C}l$. A representative number of linear plots of d/A_C against $1/(A_\text{C})^{\frac{1}{2}}$ are shown in Figure 8 for a selection of different dibenzo-$3n$-crown-n ether hosts. The association constants (K_a) and derived $-\Delta G°$ values, obtained from all the plots, which afforded straight lines, are recorded in Table 6. Obtaining of a linear plot is, of course,
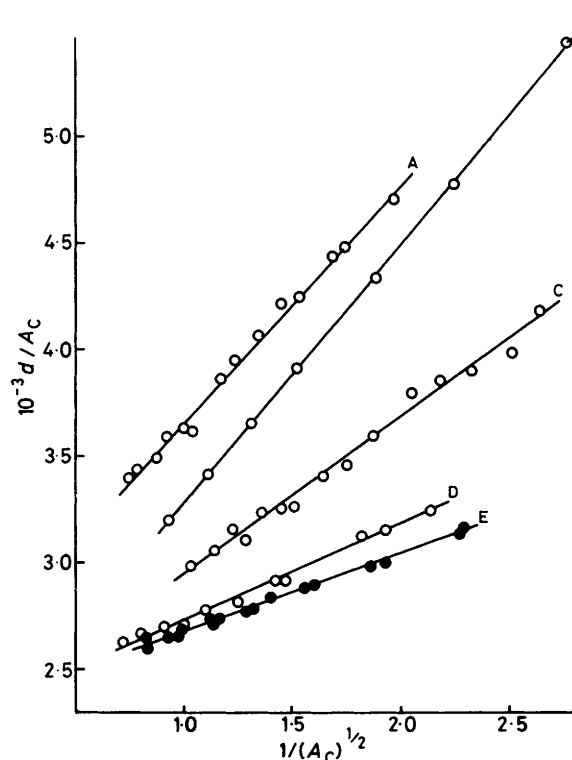
Figure 8. A representative number of the linear plots of d/A_C against $1/(A_\text{C})^{\frac{1}{2}}$ for a selection of different hosts. See Table 6 for an explanation of the plots A, B, C, D, and E

Table 6. Association constants (K_a) and derived free energies of complexation $(\Delta G°)$ for 1:1 complex formation in solution at 25.5 °C between diquat bis(hexafluorophosphate) (2) and various molecular receptors

Molecular receptor	Solvent	Data points	Plot[a]	Correlation coefficient	K_a/M^{-1}	$-\Delta G°/\text{kcal mol}^{-1}$
DB27C9 (13)	Me$_2$CO	16[b]		0.991	410 ± 60	3.57 ± 0.08
DB30C10 (14)	Me$_2$CO	17[c]	E	0.996	17 500 ± 1 100	5.79 ± 0.05
DB30C10 (14)	MeCN	15	C	0.994	4 100 ± 400	4.92 ± 0.05
DB33C11 (15)	Me$_2$CO	11[d]	D	0.995	10 800 ± 800	5.52 ± 0.05
DB36C12 (16)	Me$_2$CO	14[e]	A	0.996	2 000 ± 200	4.52 ± 0.05
DN30C10(27)	MeCN	7	B	1.000	1 390 ± 30	4.29 ± 0.01

[a] See Figure 8. [b] Concentration range, 3—13 × 10^{-3}M. [c] Concentration range, 0.6—3.8 × 10^{-3}M. [d] Concentration range, 0.7—5 × 10^{-3}M. [e] Concentration range, 1—7 × 10^{-3}M.

consistent with 1:1 complexation between the hosts listed in Table 6 and diquat bis(hexafluorophosphate) (2) over a certain concentration range. For 1:1 complexation between (2) and DB30C10 (14) in acetontrile, where 15 data points were obtained, there is a highly satisfactory correlation (plot C in Figure 8) between d/A_C and $1/(A_C)^{\frac{1}{2}}$. With fewer (i.e., 7) data points, the correlation (plot B in Figure 8) between the same variables was perfect for the 1:1 complex formed between (2) and DN30C10 (27) in acetonitrile.

The situation was not so straightforward, however, with experiments carried out in acetone as solvent. (The choice of this solvent was governed by our desire to be able to relate stability constant measurements to the ^{1}H n.m.r. spectroscopic investigations carried out in CD_3COCD_3.) For example, in the case of the complexation between (2) and DB36C12 (16) the d/A_C against $1/(A_C)^{\frac{1}{2}}$ plot is linear (plot A in Figure 8) over the concentration range 1—7 $\times$ 10^{-3}M but deviates from linearity at concentrations >7 $\times$ 10^{-3}M to give eventually another straight line but this time with a negative slope. Although the reasons for this deviation are not understood, they obviously reflect the breakdown of the 1:1 model at high concentrations of the guest and host. The data obtained for the complexation of (2) with DB27C9 (13), DB30C10 (14), and DB33C11 (15) also exhibit the same kind of behaviour at high concentrations and the relevant straight line plots (D and E) in Figure 8 relate to the concentration ranges indicated in Table 6. When the complexation experiment was performed repeatedly on equimolar amounts of (2) and DB24C8 (11), non-linear plots of d/A_c against $1/(A_C)^{\frac{1}{2}}$ were obtained without exception. Consequently, a treatment to test for 2:1 (guest:host) stoicheiometry was devised in a manner similar to that described previously for 1:1 complexation. By defining an equilibrium constant, K_a', [equation (11)], and assuming that stoicheiometries other than

$$K_a' = \frac{[2:1 \text{ complex}]}{[\text{diquat}^{2+}.2PF_6^-]^2[\text{DB24C8}]} \qquad (11)$$

2:1 (guest:host) are not significant, we obtain equation (12) where $A_C' = A - 2\varepsilon_D dl$, $\varepsilon_C' = \varepsilon_X - 2\varepsilon_D$, A is the measured

$$\frac{d}{A_C'} = \left(\frac{1}{4K_a'\varepsilon_C'l}\right)^{1/3} \cdot \frac{1}{(A_C')^{2/3}} + \frac{1}{\varepsilon_C'l} \qquad (12)$$

absorbance, ε_D is the molar absorptivity for diquat, d is the total concentration of DB24C8, $2d$ is the total concentration of diquat, l is the path length, and ε_X is the molar absorptivity for the 2:1 complex. Thus, for a series of solutions of different concentration d, but with $[\text{diquat}^{2+}.2PF_6^-]:[\text{DB24C8}]$ equal to 2 throughout, a plot of d/A_C' against $1/(A_C')^{2/3}$ should be linear with the slope of the line equal to $(1/4K_a'\varepsilon_C'l)^{1/3}$ and intercept on the d/A_C' axis equal to $1/\varepsilon_C'l$. A straight line plot was obtained with 7 data points in the concentration (d) range 1.2—4.3 $\times$ 10^{-3}M. The equilibrium constant, K_a', calculated from this plot was 385 000 $\pm$ 38 000 M^{-2}. While this value may be regarded as high, it should be appreciated that it is effectively the product of the association constants for two 1:1 complexations.

The determination of the equilibrium constants for the association between diquat bis(hexafluorophosphate) (2) and the series of dibenzo-3n-crown-n ethers (n = 8—12) (11), (13)—(16) in acetone (i) provides convincing evidence for the stoicheiometry of the solution complexes, (ii) allows the calculation of free energies of complexation, and (iii) confirms the qualitative ^{1}H n.m.r. spectroscopic and optical studies which suggest that the complexation between the diquat dication and a dibenzo-3n-crown-n ether should be optimal when n = 10, i.e., when the crown ether is DB30C10 (14).

The association constants, K_a, and derived free energies of

complexation, ΔG°, are listed in Table 6 for the series of dibenzo-3n-crown-n ethers (n = 9—12) (13)—(16) which give 1:1 complexes with the diquat dication in acetone. A plot of $-\Delta G^\circ$ versus n is given in Figure 2. In addition to the striking similarity between this plot and the one in which the qualitative optical studies in acetonitrile are summarised, the marked dependence of $-\Delta G^\circ$ on n is also clearly illustrated. The modulus of ΔG° is a maximum when n = 10, and the values of ΔG° when n = 11, and when n = 12, may be conveniently discussed in terms of perturbations to the 1:1 complex formed between the diquat dication and DB30C10 (14), i.e., when n = 10. We have suggested (vide infra) that ^{1}H n.m.r. spectroscopic studies support a description of the structure of the 1:1 complex between the diquat dication and DB30C10 (14) in solution which is similar to that of the same complex in the solid state. Both in solution and in the solid state, there will be a conflict between (i) that U-shaped conformation of DB30C10 (14) which is required to maximise the intermolecular host–guest binding energy, and (ii) that conformation which minimises all components of steric and electronic strain within the polyether chains of the crown ether itself.

The intermolecular host–guest binding energy in the [diquat.DB30C10]$^{2+}$ complex presumably arises from charge transfer, hydrogen bonding, Coulombic, and van der Waals interactions, all stabilising features which are expected to be sensitive to the geometrical relationship between the bipyridinium moiety of the diquat dication and the two benzo-rings of DB30C10 (14). Imagine then, the extension of one polyether chain in the 1:1 solution complex between the diquat dication and DB30C10 (14) by one bismethyleneoxy unit to give the 1:1 complex between the diquat dication and DB33C11 (15). As indicated by the chemical shift trends in the ^{1}H n.m.r. spectra (Figure 7), there appears to be a small but definite change in the geometrical relationship between the aromatic rings as this progression is made. There is also a change (Table 6 and Figure 2) in the host–guest binding energy as indicated by the reduction in the absolute value of ΔG° for the [diquat.DB33C11]$^{2+}$ complex relative to that for the [diquat.DB30C10]$^{2+}$ complex. These experimental trends are even more manifest when a further bismethyleneoxy unit is formally inserted into the other polyether chain of DB30C10 (14) to give the [diquat.DB36C12]$^{2+}$ complex. Clearly, the reduction in the intermolecular host–guest binding energy is a composite phenomenon involving all the components of intermolecular stabilisation listed above, together perhaps with increased torsional strain in the lengthened polyether chains, and possibly also undesirable solvation effects.

An attempt to portray the situation diagrammatically is made in Figure 9. Figure 9(a) presents a schematic representation of the 1:1 complex between the diquat dication and DB30C10 (14). It is drawn in such a way as to represent the situation of near optimum hydrogen-bond formation involving the polyether chains and where there is a maximum overlap between the two benzo-rings of DB30C10 (14) and the bipyridinium ring system of the diquat dication. Figure 9(b) represents the situation where both polyether chains have been extended by the inclusion of a bismethyleneoxy unit and as such it represents the 1:1 complex between the diquat dication and DB36C12 (16). Here, the bipyridinium ring system is displaced towards the polyether chains whose loops are larger than is desirable for optimum hydrogen-bond formation. However, judging from the plots in Figures 2, the decrease in the binding of the diquat dication by DB3nCn hosts in the range n = 10—12 is gradual.

The free energy of complexation for the 1:1 complex between DB27C9 (13) and the diquat dication is significantly less (Table 6 and Figure 2) than that for the [diquat.DB30C10]$^{2+}$ complex. We assume that DB27C9 (13) is too small to form a U-shaped

(a)

(b)

(c)

(d)

$\equiv$ **Benzo rings** $\equiv$ **Diquat dication** $\equiv$ **Polyether chains**
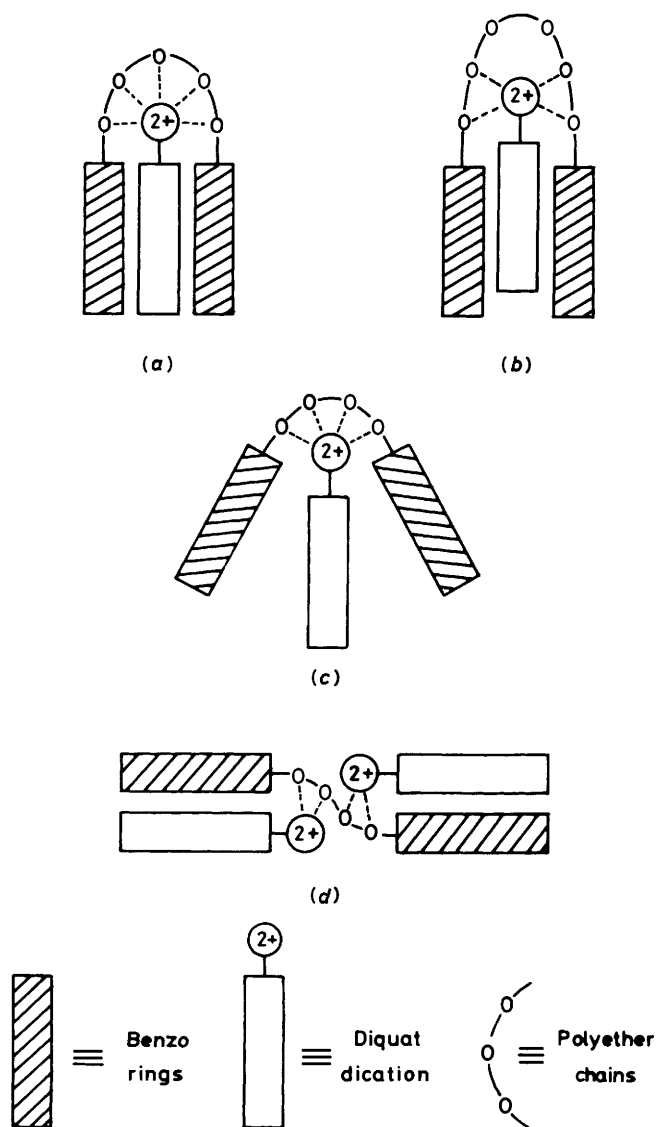
Figure 9. A schematic representation of the complexes formed between the diquat dication and (a) DB30C10 (14), (b) DB36C12 (16), (c) DB27C9 (13), and (d) DB24C8 (11). [It should be emphasised that the diagram in (c) is a symmetrical representation of the case of impaired charge-transfer stabilisation: a distorted asymmetric structure with one of the host benzo-rings lying parallel to the bipyridinium ring system and the other benzo-ring unable to reach far enough round for good overlap is another possible representation (see reference 2). Although the symmetrical representation may not correspond to the energetically most favourable superstructure, it probably represents the average superstructure which exists in geometrical terms in solution]

cavity, as shown for DB30C10 (14) in Figure 9(a) and that it forms a V-shaped cavity as illustrated in Figure 9(c). In the [diquat.DB27C9]$^{2+}$ complex, the diquat dication can only bind strongly to one of the benzo-rings of the host [although exchange between the two binding sites is fast on the ^{1}H n.m.r. time scale as indicated by the equivalence of the two sets of benzo-protons in the ^{1}H n.m.r. spectrum of a 1:1 mixture of diquat bis(hexafluorophosphate) (2) and DB27C9 (13)] and this results in a dramatic reduction in the free energy of complexation (see Figure 2).

Presumably, DB24C8 (11) is so small that it cannot even form a V-shaped cavity and it becomes energetically favourable for it

to form a 2:1 (guest:host) complex, the cost in entropy, as a result of the formation of a termolecular rather than a bimolecular complex, being outweighed by the gain in enthalpy when two diquat dications bind to the host, one to each benzo-ring, perhaps as indicated diagrammatically in Figure 9(d). Surely, it is not coincidental that the free energy of formation (-7.6 kcal mol^{-1}) for the 2:1 complex between the diquat dication and DB24C8 (11) is approximately twice that (-3.6 kcal mol^{-1}) for the formation of the 1:1 complex between the diquat dication and DB27C9 (13). The observation that the $-\Delta G°$ value for the 2:1 complex is greater by a factor of a little more than two may reflect the fact that, in the 'open' structure illustrated in Figure 9(d), there is greater scope for optimum geometrical overlap to be attained between the bipyridinium ring systems of the diquat dications and the benzo-rings of DB24C8 (11). In the V-shaped cavity of the [diquat·DB27C9]$^{2+}$ complex [Figure 9(c)], optimal overlap between the diquat dication and the benzo-rings is unlikely to be achieved simply because of the greatly reduced size of the polyether cavity.

In the discussion given above, the variation of the free energy of complexation as a function of crown ether ring size has been discussed almost solely in terms of guest–host binding energy (enthalpy). We have paid no attention to the roles of the solvent and/or the counterions simply because no information is available. As far as counterions are concerned, the mathematical models used to determine the free energies of complexation made no assumptions. However, it is likely that any cationic complex–counterion interaction will be most significant in the case of the termolecular, formally tetracationic, [(diquat)$_2$.DB24C8]$^{4+}$ complex. In connection with solvent effects, we note that it proved impossible to record the ^{1}H n.m.r. spectrum of a 1:1 mixture of diquat bis(hexafluorophosphate) (2) and DB18C6 (10) in acetone. In general, the dibenzo-3n-crown-n ethers were only sparingly soluble in acetone and it may be that there is some variation in the host solvation energies in acetone. However, such a variation might be expected to make only a very small contribution to the free energies of complexation. That the free energy of complexation (-4.9 kcal mol^{-1}) for the 1:1 complex between the diquat dication and DB30C10 (14) in acetonitrile is less (Table 6) than that (-5.8 kcal mol^{-1}) for the same complex in acetone is not surprising. Presumably, the difference arises from (i) the greater solvent polarity of acetonitrile, and more importantly perhaps, from (ii) competitive binding between acetonitrile and DB30C10 (14), cf. the formation[30] of molecular complexes between acetonitrile and 18-crown-6 and its derivatives.

If we make the assumption that the structure of the 1:1 complex between the diquat dication and DN30C10 (27) is similar to that of the 1:1 complex between the diquat dication and DB30C10 (14) in that the relative dispositions of the bipyridinium ring system and the aryl oxygen atoms are identical, then we can expect a reduction in the charge-transfer binding in the [diquat.DN30C10]$^{2+}$ complex relative to that in the [diquat.DB30C10]$^{2+}$ complex on account of the impaired π-donor–π-acceptor overlap. This is because, although the π-donor orbitals are higher in energy in the case of the naphtho-ring systems, and so are expected to interact more favourably with the unoccupied π-acceptor orbitals in the diquat dication, efficient electrostatic stabilisation of the dication leads to overlap of the π-donor rings with the π-acceptor ring in a geometrically unfavourable manner, thus reducing the strength of the charge-transfer interactions. Conversely, if there is a reorganisation of the superstructure of the [diquat.DN30C10]$^{2+}$ complex in such a way that π–π overlap is maximised, then there will be a reduction in that part of the guest–host binding energy which is due to hydrogen bonding and other electrostatic interactions. These interpretations are consistent with the relative ordering (Table 6) of the

free energies of formation for the two complexes. An investigation of the binding of the diquat dication to a range of DN3nCn hosts similar to that reported in this paper for DB3nCn hosts would help to test these tentative proposals.

An attempt to shed light on the relative importance of charge transfer *versus* other forms of binding in the [diquat.DB3nCn]$^{2+}$ complexes by employing the 28-membered ring compound (30) as a host for the diquat dication was frustrated by the poor solubility of (30) in nearly all solvents even in the presence of diquat bis(hexafluorophosphate) (2). No evidence for complexation of the diquat dication was obtained.

This investigation has opened the way for the design and synthesis of more highly ordered, and elaborate, receptor molecules for the diquat dication and related guest species.

Experimental

Tetrahydrofuran was refluxed over sodium–benzophenone and then distilled under nitrogen. T.l.c. was carried out on glass plates (20 × 5 cm) coated with Merck 7736 Kieselgel 60H. Developed plates were air-dried, scrutinised under a u.v. lamp, and then sprayed with cerium(IV) sulphate–sulphuric acid reagent and heated at *ca.* 100 °C. Column chromatography was performed[31] at the bench on silica gel 60 (40—63 µm, Merck 9385). M.p.l.c. was carried out on a Waters PrepLC/System 500A. Melting points were determined with a Reichert hot-stage apparatus and are uncorrected. Microanalyses were carried out by the University of Sheffield microanalytical service. High-resolution mass spectra were obtained from a Kratos MS 80 instrument. U.v. spectra were recorded on a Perkin-Elmer 402 ultraviolet–visible spectrophotometer. ^{1}H N.m.r. spectra (tetramethylsilane as lock and internal standard) were recorded with Bruker WH400 (400 MHz) and Perkin-Elmer R34 (220 MHz) spectrometers.

Dibenzo-18-crown-6[3] (10) and dibenzo-24-crown-8[3] (11) were obtained from Aldrich.

6,7-Dihydrodipyrido[1,2-a:2',1'-c]*pyrazidinium* *Bis(hexafluorophosphate)* (*Diquat Bishexafluorophosphate*)[32] (2).—Anhydrous diquat dibromide (937 mg, 2.72 mmol) was dissolved in water (5 ml) and the solution was filtered. This aqueous solution was added to a solution of sodium hexafluorophosphate (915 mg, 5.45 mmol) in water (5 ml) which had also been filtered. A cream-coloured precipitate was formed immediately. The mixture was stored overnight at 0 °C before the precipitate was filtered off, washed with a *small* amount [since the bis(hexafluorophosphate) salt is sparingly soluble] of water, and dried under vacuum in the presence of phosphorus pentaoxide–potassium hydroxide during several days with repeated changes of the desiccant to afford diquat bis(hexafluorophosphate)(2)(304 mg,24%),m.p. > 300 °C,but with some decomposition at *ca.* 250 °C (Found: C, 30.5; H, 2.4; N, 6.0. Calc. for C$_{12}$H$_{12}$F$_{12}$N$_2$P$_2$: C, 30.4; H, 2.55; N, 5.9%); δ (CD$_3$COCD$_3$; 220 MHz) 5.66 (4 H, s, methylene protons), 8.56 (2 H, br t, *J* 7 Hz, 5-H, and 5'-H), 9.06 (2 H, t, *J* 8 Hz, 4-H and 4'-H), 9.19 (2 H, d, *J* 7.8 Hz, 3-H and 3'-H), and 9.44 (2 H, d, *J* 6.1 Hz, 6-H and 6'-H). Although indicated to be pure by elemental analysis, solutions of the salt in acetone were very slightly hazy. Accordingly, the salt was dissolved in acetone and filtered through a tightly packed cotton-wool plug. The filtrate was evaporated to give a sample of diquat bis(hexafluorophosphate) (2) suitable for spectroscopic studies. Higher yields of the salt were obtained by mixing much more concentrated aqueous solutions of diquat dibromide and sodium hexafluorophosphate. However, the purity of the salt was somewhat less as indicated by the increased amount of acetone-insoluble material.

Although the preparation of diquat bis(hexafluorophosphate) (2) by the metathesis between diquat dibromide and ammonium

hexafluorophosphate in aqueous solution has been reported[32] recently, no analytical or spectroscopic data in support of its identity are given.

3-Oxapentane-1,5-diylbis(toluene-p-sulphonate)[6,33] (*Diethyleneglycol Bistosylate*) (3).—The preparation of this bistosylate(3) has been described by us[33] and others[6] previously.

3,6-Dioxaoctane-1,8-diylbis(toluene-p-sulphonate) (*Triethyleneglycol Bistosylate*)[6] (4).—Toluene-*p*-sulphonyl chloride (126 g) was added portionwise over a period of 30 min to a solution of triethylene glycol (50 g) in dry pyridine (250 ml) cooled to −5 °C in a salt–ice bath. The temperature of the reaction mixture was kept below 5 °C during the addition. After stirring for a further 2 h, the reaction mixture was filtered to remove precipitated pyridinium chloride and the filtrate was poured onto crushed ice (400 g). Concentrated hydrochloric acid was added to neutralise the pyridine and the white precipitate was filtered off under suction and washed with water (5 × 400 ml) and ice-cold ethanol (50 ml). The crude product was recrystallised from ethanol to afford colourless plates of triethyleneglycol bistosylate (4) (73 g, 43%), m.p. 77—80 °C, lit.,[6] 78 °C [Found: *M* (mass spectrometry), 458; C, 52.1; H, 5.9; S, 14.2%. Calc. for C$_{20}$H$_{26}$O$_8$S$_2$: *M*, 458; C, 52.4; H, 5.7; S, 14.0%]; δ (CDCl$_3$; 220 MHz) 2.37 (6 H, s, 2 × Ar*Me*), 3.50 (4 H, s, OCH$_2$CH$_2$O), 3.62 (4 H, t, *J* 5 Hz, 2 × OC*H$_2$*CH$_2$OTs), 4.06 (4 H, t, *J* 5 Hz, 2 × OCH$_2$C*H$_2$*OTs), and 7.25 and 7.72 (8 H, 2 × A$_2$B$_2$ systems, J_{AB} 8 Hz, aromatic protons).

3,6,9-Trioxaundecane-1,11-diylbis(toluene-p-sulphonate) (*Tetraethyleneglycol Bistosylate*)[6] (5).—Tetraethyleneglycol (58.2 g) was treated with toluene-*p*-sulphonyl chloride (127 g) in dry pyridine (200 ml) as described previously for the tosylation of triethylene glycol. The crude product obtained after work-up was subjected to column chromatography on silica gel using diethyl ether as eluant to afford pure tetraethyleneglycol bistosylate (5) (84.5 g, 56%) as an oil [Found: *M* (mass spectrometry), 502. Calc. for C$_{22}$H$_{30}$O$_9$S$_2$: *M*, 502]; δ (CDCl$_3$; 220 MHz) 2.42 (6 H, s, 2 × Ar*Me*), 3.55 (8 H, s, 2 × OCH$_2$CH$_2$O), 3.67 (4 H, t, *J* 5 Hz, 2 × C*H$_2$*CH$_2$OTs), 4.16 (4 H, t, *J* 5 Hz, 2 × OCH$_2$C*H$_2$*OTs), and 7.35 and 7.80 (8 H, 2 × A$_2$B$_2$ systems, J_{AB} 9 Hz, aromatic protons).

3,6,9,12-Tetraoxatetradecane-1,14-diylbis(toluene-p-sulphonate) (*Pentaethyleneglycol Bistosylate*)[33] (6).—Pentaethyleneglycol (26.3 g) was treated with toluene-*p*-sulphonyl chloride (52.6 g) in dry pyridine (150 ml) as described previously for the tosylation of triethyleneglycol. The crude product obtained after work-up was subjected to medium-pressure liquid chromatography on silica gel using ethyl acetate–light petroleum (b.p. 60—80 °C) (4:1) as eluant to afford pentaethyleneglycol bistosylate (6) (62.2 g, 75%) as an oil [Found: *M* (mass spectrometry), 546; C, 52.8; H, 6.1; S, 11.8%. Calc. for C$_{24}$H$_{34}$O$_{10}$S$_2$: *M*, 546; C, 52.7; H, 6.3; S, 11.7%]; δ (CDCl$_3$; 220 MHz) 2.44 (6 H, s, 2 × Ar*Me*), 3.58 and 3.60 (12 H, 2 × s, 3 × OCH$_2$CH$_2$O), 3.69 (4 H, t, *J* 5 Hz, 2 × OC*H$_2$*-CH$_2$OTs), 4.17 (4 H, t, *J* 5 Hz, 2 × OCH$_2$C*H$_2$*OTs), and 7.35 and 7.80 (8 H, 2 × A$_2$B$_2$ systems, J_{AB} 9 Hz, aromatic protons).

6,7,9,10,12,13,15,16,18,19-Decahydrobenzo[1,4,7,10,13,16]-*hexaoxacyclo-octadiene* (*Benzo-18-crown-6*)[3] (9).—Catechol (7) (5.0 g) in dry tetrahydrofuran (60 ml) was stirred at room temperature while sodium hydride (5.2 g; 50% dispersion in oil) was added. After 1.5 h, pentaethyleneglycol bistosylate (6) (24.8 g) in dry tetrahydrofuran (70 ml) was added dropwise with stirring during 2 h. The reaction mixture was heated under reflux for 3 h, further portions (1.0 g and 0.5 g, respectively) of catechol (7) and sodium hydride were added, and refluxing was

continued for an additional 4 h. On cooling, water (200 ml) was added, and the crude product was obtained after extraction with chloroform. The crude product was washed with pentane and then distilled under vacuum (0.005 mmHg), giving a fraction which distilled between 170 and 190 °C and crystallised in cooling to afford benzo-18-crown-6 (9) (5.7 g, 40%), m.p. 40—41 °C (lit.,[3] 43—44 °C); δ (CD$_2$Cl$_2$; 220 MHz) 3.58—3.80 (12 H, m, with s at δ 3.62, γ-CH$_2$, δ-CH$_2$, and ε-CH$_2$), 3.82—3.95 (4 H, m, β-CH$_2$), 4.09—4.20 (4 H, m, α-CH$_2$), and 6.88 (4 H, s, C$_6$H$_4$).

o-Benzyloxyphenol[8] (8).—Sodium (7.0 g) was dissolved in dry methanol (110 ml) and the methanolic solution of sodium methoxide was added under nitrogen with stirring to catechol (7) (33 g) in dry methanol (75 ml). After allowing the mixture to stand at room temperature for 15 min, benzyl chloride (34.5 ml) in dry methanol (75 ml) was added dropwise during 1.5 h. The reaction mixture was heated under reflux for 2 h, cooled, acidified with concentrated hydrochloric acid, filtered to remove sodium chloride, and concentrated to afford a residual oil. After partitioning between water and chloroform, the crude product was distilled under vacuum (0.05 mmHg) to give *o*-benzyloxyphenol (8) (22.1 g, 37%), b.p. 107—116 °C (lit.,[8] 173—174 °C at 13 mmHg); δ (CDCl$_3$; 220 MHz) 5.01 (2 H, s, benzylic methylene protons), 5.70 (1 H, s, OH), 6.70—6.96 (4 H, m, C$_6$H$_4$), and 7.25—7.40 (5 H, br s, C$_6$H$_5$).

1,8-Bis-(o-benzyloxyphenoxy)-3,6-dioxaoctane (17).—The phenol (8) (10.2 g) dissolved in dry tetrahydrofuran (40 ml) was added at room temperature under nitrogen to a stirred suspension of sodium hydride (1.8 g) in dry tetrahydrofuran (30 ml). After stirring the mixture at 45 °C for 1 h, triethyleneglycol bistosylate (4) (12.1 g) in dry tetrahydrofuran (100 ml) was added during 1.5 h. The reaction mixture was heated under reflux for 16 h, cooled, quenched with water, and extracted with chloroform. The crude product was subjected to column chromatography on silica gel using ethyl acetate–light petroleum (b.p. 60—80 °C) (3:7 followed by 1:1) as eluant yielding 1,8-*bis*-(o-*benzyloxyphenoxy*)-3,6-*dioxaoctadecane* (17) (9.7 g, 74%), m.p. 50.5—52 °C [Found: M (mass spectrometry), 514; C, 74.7; H, 6.7%. C$_{32}$H$_{34}$O$_6$ requires M, 514; C, 74.7; H, 6.7%]; δ (CDCl$_3$; 220 MHz) 3.73 (4 H, s, γ-CH$_2$), 3.87 (4 H, t, J 5.0 Hz, β-CH$_2$), 4.20 (4 H, t, J 5.0 Hz, α-CH$_2$), 5.11 (4 H, s, benzylic methylene protons), 6.85—6.98 (8 H, m, 2 × C$_6$H$_4$), and 7.23—7.48 (10 H, m, 2 × C$_6$H$_5$).

1,11-Bis-(o-benzyloxyphenoxy)-3,6,9-trioxaundecane (18).—Employing reaction conditions and a work-up procedure similar to those described for the preparation of the dibenzyl ether (17), reaction of the phenol (8) (11.0 g), sodium hydride (1.64 g), and tetraethyleneglycol bistosylate (5) (13.8 g) in dry tetrahydrofuran (100 ml) afforded a crude product (14.7 g). Column chromatography on silica gel using ethyl acetate–light petroleum (b.p. 60—80 °C) (3:2) as eluant yielded pure 1,11-*bis*-(o-*benzyloxyphenoxy*)-3,6,9-*trioxaundecane* (18) as an oil (11.4 g, 75%) (Found: C, 72.9; H, 7.0. C$_{34}$H$_{38}$O$_7$ requires C, 73.1; H, 6.9%); δ (CDCl$_3$; 400 MHz) 3.58—3.63 (4 H, m, δ-CH$_2$), 3.68—3.73 (4 H, m, γ-CH$_2$), 3.84 (4 H, t, J 5.0 Hz, β-CH$_2$), 4.17 (4 H, t, J 5.0 Hz, α-CH$_2$), 5.10 (4 H, s, benzylic methylene protons), 6.85—6.98 (8 H, m, 2 × C$_6$H$_4$), and 7.28—7.48 (10 H, m, 2 × C$_6$H$_5$).

1,14-Bis-(o-benzyloxyphenoxy)-3,6,9,12-tetraoxatetradecane (19).—Employing reaction conditions and a work-up procedure similar to those described for the preparation of the dibenzyl ether (17), reaction of the phenol (8) (10.2 g), sodium hydride (1.8 g), and pentaethyleneglycol bistosylate (13.9 g) in dry tetrahydrofuran (200 ml) yielded a crude product (14.2 g). Column chromatography on silica gel using ethyl acetate–light

petroleum (b.p. 60—80 °C) (3:2 followed by 4:1) as eluant yielded pure 1,14-*bis*-(o-*benzyloxyphenoxy*)-3,6,9,12-*tetraoxatetradecane* (19) (11.3 g, 74%), m.p. 49.5—50.5 °C [Found: M (mass spectrometry), 602; C, 71.7; H, 7.0%. C$_{36}$H$_{42}$O$_8$ requires M, 602; C, 71.7; H, 7.0%]; δ (CDCl$_3$; 220 MHz) 3.56—3.68 (8 H, m with s at δ 3.60, δ-CH$_2$ and ε-CH$_2$), 3.69—3.79 (4 H, m, γ-CH$_2$), 3.87 (4 H, t, J 5.0 Hz, β-CH$_2$), 4.20 (4 H, t, J 5.0 Hz, α-CH$_2$), 3.69—3.79 (4 H, m, α-CH$_2$), 3.87 (4 H, t, J 5.0 Hz, β-CH$_2$), 4.20 (4 H, t, J 5.0 Hz, α-CH$_2$), 5.11 (4 H, s, benzylic methylene protons), 6.85—7.00 (8 H, m, 2 × C$_6$H$_4$), and 7.25—7.55 (10 H, m, 2 × C$_6$H$_5$).

1,8-Bis-(o-hydroxyphenoxy)-3,6-dioxaoctane (20).—The dibenzyl ether (17) (9.4 g) was dissolved in methanol (250 ml) containing dichloromethane (50 ml) and subjected to hydrogenolysis over 10% palladium on carbon (250 mg). The product (20) (6.0 g, 98%) was employed in the following cyclisation step without further purification. δ (CDCl$_3$; 220 MHz) 3.72 (4 H, s, γ-CH$_2$), 3.80—3.87 (4 H, m, β-CH$_2$), 4.15—4.23 (4 H, m, α-CH$_2$), 6.40 (2 H, br s, 2 × OH), and 6.75—7.00 (8 H, m, 2 × C$_6$H$_4$).

1,11-Bis-(o-hydroxyphenoxy)-3,6,9-trioxaundecane (21).—The dibenzyl ether (18) (7.8 g) was dissolved in methanol (100 ml) containing dichloromethane (3 ml) and subjected to hydrogenolysis over 10% palladium on carbon (500 mg). The product (21) (5.2 g, 98%) was employed in the following cyclisation step without further purification. δ (CDCl$_3$; 220 MHz) 3.60—3.75 (8 H, br s, γ-CH$_2$ and δ-CH$_2$), 3.75—3.90 (4 H, m, β-CH$_2$), 4.05—4.25 (4 H, m, α-CH$_2$), 6.45 (2 H, br s, 2 × OH), and 6.70—7.00 (8 H, m, 2 × C$_6$H$_4$).

1,14-Bis-(o-hydroxyphenoxy)-3,6,9,12-tetraoxatetradecane (22).—The dibenzyl ether (19) (8.4 g) was dissolved in methanol–dichloromethane (95:5) (100 ml) and subjected to hydrogenolysis over 10% palladium on carbon (500 mg). The product (22) (5.6 g, 95%) was employed in the following cyclisation step without further purification [Found: M (mass spectrometry), 422. C$_{22}$H$_{30}$O$_8$ requires M, 422]; δ (CDCl$_3$; 220 MHz) 3.60—3.77 (12 H, m with s at δ 3.68, γ-CH$_2$, δ-CH$_2$, and ε-CH$_2$), 3.77—3.95 (4 H, m, β-CH$_2$), and 4.10 (4 H, m, α-CH$_2$), 6.70—7.00 (8 H, m, 2 × C$_6$H$_4$), and 7.08 (2 H, br s, 2 × OH).

6,7,9,10,17,18,20,21,23,24-Decahydrodibenzo[b,k]-[1,4,7,10,13,16,19]-heptaoxacycloheneicosin (Dibenzo-21-crown-7)[3] (12).—The diphenol (20) (5.8 g), dissolved in dry tetrahydrofuran (75 ml), was stirred with sodium hydride (2.2 g) under nitrogen at 60 °C for 1 h. Diethyleneglycol bistosylate (3) (8.0 g), dissolved in dry tetrahydrofuran (100 ml), was added dropwise with stirring during 2 h. The reaction mixture was heated under reflux for 72 h. A standard work-up procedure involving partitioning between a dichloromethane and an aqueous phase afforded a crude product. Column chromatography on silica gel using ethyl acetate–light petroleum (b.p. 60—80 °C) (7:3) as eluant led to the isolation of a crystalline sample of dibenzo-21-crown-7 (12) (2.4 g, 34%) after crystallisation from methanol–light petroleum (b.p. 60—80 °C), m.p. 103.5—104.5 °C (lit.,[3] 106.5—107.5 °C) [Found: M (mass spectrometry), 404; C, 65.1; H, 6.9%. Calc. for C$_{22}$H$_{28}$O$_7$: M, 404; C, 65.3; H, 7.0%]; δ (CDCl$_3$; 220 MHz) 3.80—3.95 (8 H, m, with s at δ3.84, β'-CH$_2$ and γ'-CH$_2$ protons), 4.01 (4 H, t, J 5.0 Hz, β-CH$_2$), 4.10—4.25 (8 H, m, α-CH$_2$ and α'-CH$_2$), and 6.89 (9 H, s, 2 × C$_6$H$_4$).

6,7,9,10,12,13,20,21,23,24,26,27,29,30-Tetradecahydrodibenzo-[b,n][1,4,7,10,13,16,19,22,25]nonaoxacycloheptacosin (Dibenzo-27-crown-9)[7] (13).—The diphenol (21) (2.5 g), dissolved in dry tetrahydrofuran (75 ml), was stirred with sodium hydride

(480 mg) under nitrogen at 55 °C for 1 h. Triethyleneglycol bistosylate (4) (3.33 g), dissolved in dry tetrahydrofuran (75 ml), was added dropwise with stirring during 2 h. Stirring was continued for 4 h at 55 °C and then for 16 h at room temperature. A standard work-up procedure involving partitioning between a chloroform and an aqueous phase afforded a crude product (3.2 g). Column chromatography on silica gel using diethyl ether–ethanol (94:6) as eluant led to the isolation of a crystalline sample of dibenzo-27-crown-9 (13) (1.75 g, 54%), m.p. 56—57 °C (lit.,[7] 81.5—82.0 °C) [Found: M (mass spectrometry), 492; C, 63.6; H, 7.4%. $C_{26}H_{36}O_9$ requires M, 492; C, 63.4; H, 7.4%); δ (CDCl$_3$; 220 MHz) 3.67—3.80 (8 H, m, γ′-CH$_2$ and δ′-CH$_2$), 3.81 (4 H, s, γ-CH$_2$), 3.86—3.94 (8 H, m, β-CH$_2$ and β′-CH$_2$), 4.12—4.22 (8 H, m, α-CH$_2$ and α′-CH$_2$), and 6.88 (8 H, s, 2 × C$_6$H$_4$).

6,7,9,10,12,13,15,16,23,24,26,27,29,30,32,33-*Hexadecahydro-dibenzo[b,q][1,4,7,10,13,16,19,22,25,28]decaoxacyclotriacontin (Dibenzo-30-crown-10)*[3] (14).—The diphenol (21) (5.1 g), sodium hydride (1.0 g), and tetraethyleneglycol bistosylate (5) (6.8 g) were stirred in dry tetrahydrofuran (200 ml) under nitrogen at room temperature for 1 h and then for a further 16 h at 45 °C. A standard work-up procedure involving partitioning between a chloroform and an aqueous phase afforded a crude product (6.7 g). Column chromatography on silica gel using dichloro-methane–diethyl ether (4:1) containing 1.5% ethanol as eluant led to the isolation of a crystalline sample of dibenzo-30-crown-10 (14) (1.8 g, 25%), m.p. 104—106.5 °C after recrystallisation from methanol (lit.,[3] m.p. 104—106.5 °C) (Found: C, 62.6; H, 7.7. Calc. for $C_{28}H_{40}O_{10}$: C, 62.7; H, 7.5%); δ (CDCl$_3$; 440 MHz) 3.66—3.70 (8 H, m, δ-CH$_2$), 3.75—3.80 (8 H, m, γ-CH$_2$), 3.86 (8 H, t, J 5.0 Hz, β-CH$_2$), 4.10 (8 H, t, J 5.0 Hz, α-CH$_2$), and 6.89 (8 H, s, 2 × C$_6$H$_4$).

6,7,9,10,12,13,15,16,23,24,26,27,29,30,32,33,35,36-*Octahydro-dibenzo[b,q][1,4,7,10,13,16,19,22,25,28,31]undecaoxacyclo-triacontin(Dibenzo-33-crown-11)(15).*—The diphenol (22) (2.0 g), sodium hydride (380 mg), and pentaethyleneglycol bistosylate (6) (3.1 g) were stirred in dry tetrahydrofuran (175 ml) under nitrogen at room temperature for 30 min and then heated under reflux for a further 24 h. A standard work-up procedure involving partitioning between a chloroform and an aqueous phase afforded a crude product (3.0 g). Column chromatography on silica gel using diethyl ether–ethanol (88:12) as eluant led to the isolation of a crystalline sample of dibenzo-33-crown-11 (15) (1.4 g, 48%), m.p. 63—65 °C [Found: M (mass spectrometry), 580; C, 61.9; H, 7.5%. $C_{30}H_{44}O_{11}$ requires M, 580; C, 62.1; H, 7.7%); δ (CDCl$_3$; 220 MHz) 3.27—3.46 (12 H, m with s at δ 3.32, δ-CH$_2$, δ′-CH$_2$, and ε′-CH$_2$), 3.48—3.63 (8 H, m, γ-CH$_2$ and γ′-CH$_2$), 3.75 (8 H, t, J 5.0 Hz, β-CH$_2$ and β′-CH$_2$), 4.31 (8 H, t, J 5.0 Hz, α-CH$_2$ and α′-CH$_2$), and 6.90 (8 H, s, 2 × C$_6$H$_4$).

6,7,9,10,12,13,15,16,18,19,26,27,29,30,32,33,35,36,38,39-*Eicosahydrodibenzo[b,t][1,4,7,10,13,16,19,22,25,28,31,34]-dodecaoxacyclohexatriacontin (Dibenzo-36-crown-12) (16).*—The diphenol (22) (5.2 g), sodium hydride (900 mg), and pentaethyleneglycol bistosylate (6) (6.7 g) were stirred in dry tetrahydrofuran (200 ml) under nitrogen at room temperature for 1 h and then for a further 16 h at 60 °C. A standard work-up procedure involving partitioning between a chloroform and an aqueous phase afforded a crude product (7.5 g). Column chromatography on silica gel using dichloromethane–diethyl ether (4:1) containing 3% ethanol as eluant led to the isolation of a crystalline sample of dibenzo-36-crown-12 (16) (2.1 g, 27%), m.p. 73.5—74 °C after recrystallisation from methanol–diethyl ether [Found: M (mass spectrometry), 624; C, 61.5; H, 7.7%. $C_{32}H_{48}O_{12}$ requires M, 624; C, 61.5; H, 7.8%); δ (CHCl$_3$; 220 MHz) 3.63—3.71 (16 H, m with s at δ 7.74, δ-CH$_2$ and ε-CH$_2$),

3.72—3.81 (8 H, m, γ-CH$_2$), 3.87 (8 H, t, J 5.0 Hz, β-CH$_2$), 4.15 (8 H, t, J 5.0 Hz, α-CH$_2$), and 6.87 (8 H, s, 2 × C$_6$H$_4$).

2-Benzyloxy-3-hydroxynaphthalene (24).—Sodium (2.9 g) was dissolved in dry methanol (40 ml) and the methanolic solution of sodium methoxide was added under nitrogen with stirring to 2,3-dihydroxynaphthalene (23) (20 g) in dry methanol. After allowing the mixture to stand at room temperature for 1 h, benzyl chloride (14.4 ml) in dry methanol (40 ml) was added dropwise during 2 h. The reaction mixture was heated under reflux for 3 h, cooled, acidified with concentrated hydrochloric acid, filtered to remove sodium chloride, and concentrated to afford a solid residue. After partitioning between water and chloroform, the crude product (30 g) was subjected to column chromatography on silica gel using diethyl ether–light petroleum (b.p. 60—80 °C) (10:90→15:85) as eluant. The monobenzyl ether (24) was isolated (6.6 g, 21%) as an oil; δ (CDCl$_3$; 220 MHz) 5.22 (2 H, s, benzylic methylene protons), 5.97 (1 H, s, OH), and 7.30—7.72 (6 H, m, aromatic protons).

1,11-Bis-(3-benzyloxy-2-naphthoxy)-3,6,9-trioxaundecane (25).—Employing reaction conditions and a work-up procedure similar to those described for the preparation of the dibenzyl ether (21), reaction of the naphthol (24) (6.6 g), sodium hydride (1.87 g), and tetraethyleneglycol bistosylate (5) (6.63 g) in dry tetrahydrofuran (170 ml) afforded a crude product (10.2 g). Column chromatography on silica gel using dichloromethane–diethyl ether–light petroleum (b.p. 60—80 °C) (20:35:45) as eluant yielded pure 1,11-bis-(3-benzyloxy-2-naphthoxy)-3,6,9-trioxaundecane (25) (4.2 g, 49%), m.p. 67—69 °C after recrystallisation from dichloromethane–diethyl ether, δ (CDCl$_3$; 220 MHz) 3.62—3.70 (4 H, m, δ-CH$_2$), 3.74—3.82 (4 H, m, γ-CH$_2$), 3.96 (4 H, t, J 5.0 Hz, β-CH$_2$), 4.29 (4 H, t, J 5.0 Hz, α-CH$_2$), 5.21 (4 H, s, benzylic methylene protons), and 7.15—7.70 (22 H, m, all aromatic protons).

1,11-Bis-(3-hydroxy-2-naphthoxy)-3,6,9-trioxaundecane (26).—The dibenzyl ether (25) (4.2 g) was dissolved in methanol–dichloromethane (7:3) (50 ml) and subjected to hydrogenolysis over 10% palladium on carbon (420 mg). The product (26) (3.0 g, 98%) was employed in the following cyclisation step without further purification [Found: M (mass spectrometry), 478. $C_{28}H_{30}O_7$ requires M, 478]; δ (CDCl$_3$–CD$_3$COCD$_3$; 220 MHz) 3.40 (2 H, br s, 2 × OH), 3.65—3.80 (8 H, m, γ-CH$_2$ and δ-CH$_2$), 3.90—4.00 (4 H, m, β-CH$_2$), 4.26—4.37 (4 H, m, γ-CH$_2$), and 7.13—7.75 (12 H, m, aromatic protons).

Di-(2,3-naphtho)-30-crown-10 (27).—The dinaphthol (26) (3.0 g), sodium hydride (450 mg), and tetraethyleneglycol bistosylate (5) (3.2 g) were stirred in dry tetrahydrofuran (150 ml) under nitrogen at room temperature for 1 h, and then for a further 16 h at 55 °C. A standard work-up procedure involving partitioning between a chloroform and an aqueous phase afforded a crude product (4.4 g). Column chromatography on silica gel using diethyl ether–dichloromethane–ethanol (55:40:5) as eluant led to the isolation, after recrystallisation from chloroform–ethyl acetate, of pure di-(2,3-naphtho)-30-crown-10 (27) (1.6 g, 23%) [Found: M (mass spectrometry), 636; C, 68.0; H, 7.23%. $C_{36}H_{44}O_{10}$ requires M, 636; C, 68.0; H, 7.23%]; δ (CDCl$_3$; 220 MHz) 3.65—3.80 (8 H, m, δ-CH$_2$), 3.80—3.90 (8 H, m, γ-CH$_2$), 3.97 (8 H, t, J 5.0 Hz, β-CH$_2$), 4.25 (8 H, t, J 5.0 Hz, α-CH$_2$), 7.09 [4 H, s, aromatic protons on C(1) and C(4) of naphtho rings], and 7.25—7.36 and 7.59—7.69 [2 × 4 H, 2 × m, aromatic protons on C(5), C(6), C(7), and C(8) of naphtho rings].

1,10-Bis-(o-benzyloxyphenoxy)decane (28).—Sodium (2.6 g) was dissolved in dry methanol (70 ml) and the methanolic solution of sodium methoxide was added under nitrogen with

stirring to the phenol (8) (15.0 g) in dry methanol (20 ml). After stirring at room temperature for 30 min, 1,10-dibromodecane (11.3 g) in dry methanol (75 ml) was added dropwise during 45 min. The reaction mixture was heated under reflux for 16 h and then further dibromide (2.8 g) was added. Refluxing was continued for an additional 4 h. Concentration afforded a residual oil, which was partitioned between water and chloroform. The chloroform layer afforded a solid, which, on crystallisation and recrystallisation from methanol, gave pure 1,10-*bis*-(o-*benzyloxyphenoxy*)*decane* (28) (9.8 g, 49%), m.p. 69—69.5 °C (Found: C, 80.4; H, 8.0. $C_{36}H_{42}O_4$ requires C, 80.3; H, 7.9%); δ (CDCl$_3$; 220 MHz) 1.20—1.54 (12 H, m, γ-CH$_2$, δ-CH$_2$, and ε-CH$_2$), 1.70—1.90 (4 H, m, β-CH$_2$), 4.00 (4 H, t, *J* 6 Hz, α-CH$_2$), 5.10 (4 H, s, benzylic methylene protons), 6.77—6.95 (8 H, m, 2 × C$_6$H$_4$), and 7.20—7.50 (10 H, m, 2 × C$_6$H$_5$).

1,10-*Bis*-(o-*hydroxyphenoxy*)*decane* (29).—The dibenzyl ether (28) (9.0 g), dissolved in ethyl acetate (40 ml), was subjected to hydrogenolysis over 10% palladium on carbon (100 mg). The crude crystalline product was recrystallised from light petroleum (b.p. 60—80 °C) to afford pure 1,10-*bis*-(o-*hydroxyphenoxy*)*decane* (29), m.p. 60—60.5 °C (Found: C, 73.9; H, 8.34. $C_{22}H_{30}O_4$ requires C, 73.7; H, 8.45%).

6,7,8,9,10,11,12,13,14,15,22,23,24,25,26,27,28,29,30,31-*Eicosahydrodibenzo*[b,p][1,12,15,26]*tetraoxacyclo-octacosin* (30).—Sodium (600 mg) was added to dry methanol (150 ml) containing the diphenol (29) (2.5 g). After allowing the mixture to stand at room temperature for 45 min, 1,10-dibromodecane (3.5 g) in dry methanol (75 ml) was added dropwise during 1 h. The reaction mixture was heated under reflux for 48 h, and then cooled in ice–water to give a precipitate of crude product (3.14 g), which could only be purified by distillation (b.p. 254 °C) under vacuum (0.08 mmHg). In this manner pure macrocycle (30) was obtained with m.p. 140—141.5 °C (lit.,[3] 137—138.5 °C) [Found: M (mass spectrometry), 496; C, 77.3; H, 9.6%. $C_{32}H_{48}O_4$ requires M, 496; C, 77.4; H, 8.8%); δ (CDCl$_3$; 220 MHz) 1.29—1.60 (24 H, m, γ-CH$_2$, δ-CH$_2$, and ε-CH$_2$), 1.71—1.88 (8 H, m, β-CH$_2$), 3.98 (8 H, t, α-CH$_2$), and 6.88 (8 H, s, 2 × C$_6$H$_4$).

Preparation of a Crystalline 1:1 *Complex between Diquat Bis*(*hexafluorophosphate*) (2) *and Dibenzo*-30-*crown*-10 (14).—(a) *General method.* Diquat bis(hexafluorophosphate) (2) (46.9 mg, 0.099 mmol) and dibenzo-30-crown-10 (14) (53.1 mg, 0.099 mmol) were dissolved in dichloromethane (1 ml) and the dark red solution was filtered to remove a small amount of insoluble material. Pentane (*ca.* 5 ml) was layered on top of the dark red filtrate and after 8 h the dark red transparent needles that formed were collected, washed with pentane, and dried to give the 1:1 *complex* (53 mg, 53%) as dark orange opaque needles with m.p. 160—163 °C (Found: C, 46.7; H, 5.19; N, 2.89. $C_{12}H_{12}F_6N_2P_2 \cdot C_{28}H_{40}O_{10} \cdot 0.33CH_2Cl_2$ requires C, 46.6; H, 5.11; N, 2.70%).

(b) *Method affording crystals suitable for* X-*ray crystallography.* Diquat bis(hexafluorophosphate) (2) (88.3 mg, 0.186 mmol) and dibenzo-30-crown-10 (14) (99.9 mg, 0.186 mmol) were dissolved in dichloromethane–methanol (3:2) (5 ml) and heptane (*ca.* 13 ml) was added. This mixture was concentrated to half its original volume. Further additions of heptane, followed by similar concentrations to half the initial volumes were repeated three times. When the mixture was allowed to cool, it afforded two phases, a lower yellow one and an upper colourless one. After standing at room temperature for 24 h, red crystals began to appear and during the following week some of these crystals grew to a size and quality suitable for X-ray structural investigation.

X-*Ray Crystal Structure Data.*—$C_{28}H_{40}O_{10} \cdot C_{12}H_{12}F_{12}$-$N_2P_2 \cdot CH_3OH$, $M_r = 1\,042.83$, deep-red needles elongated along *a*, monoclinic, *a* = 11.369(1), *b* = 22.218(5), *c* = 37.663(8) Å, β = 92.87(1)°, *U* = 9 502 Å^3, space group *P2$_1$/c*, *Z* = 8 [two crystallographically independent sets of complexes (I and II) in the asymmetric unit], $D_c = 1.46$ g cm^{-3}. The crystals rapidly desolvate and craze on removal from solution. A single crystal was therefore transferred under solution into a Lindemann glass capillary tube. Excess of the solution was carefully drawn off and the tube sealed leaving a small drop at one end of the tube to maintain a solvent vapour pressure. Refined unit-cell parameters were obtained by centring 21 reflections on a Nicolet R3m diffractometer. 9 772 Independent reflections (θ ≤ 50°) were measured with Cu-$K_α$ radiation (graphite monochromator) using the omega-scan measuring routine. Of these, 5 549 had $|F_o| > 2.5$ σ($|F_o|$) and were considered to be observed. During the data collection the orientation matrix for the crystal was automatically updated every 750 reflections so as to compensate for any small movements of the crystal within the tube. The data were corrected for Lorentz and polarisation factors; no absorption corrections were applied.

The structure was solved by direct methods. In view of the size of the structure (136 non-hydrogen atoms) care was taken in selecting a suitable starting set for the initial phase expansion. A starting set, comprising one high-probability Σ1 phase indication together with the five principal contributors to the list of negative quartets, and a further nine automatically selected terms, was chosen. The subsequent phase expansion involving a total of 16 384 permutations resulted in several phase solutions that had promising figures of merit.

Three cycles of Δ*E*-map recycling for one of these solutions revealed 48 potential atomic positions, though these gave a fairly high R_E of 0.49 for the 1 435 *E* values >1.48 used in the calculations. As several plausible molecular fragments seemed to be appearing, 39 positions were retained and a further five cycles of Δ*E*-map recycling carried out. This resulted in a considerably improved R_E of 0.35 for 91 potential atomic positions. At this stage, parts of the four PF$_6^-$ anions and the two diquat dications were clearly visible though only fragments of the two DB30C10 molecules could be seen. The remaining atomic positions were obtained from a succession of conventional Δ*F*-maps.

The non-hydrogen atoms were refined anisotropically. The refinement showed there to be severe disorder in all the PF$_6^-$ anions. These anions were idealised and refined as rigid bodies. This approach, although improving the ratio of observations to observed parameters, did produce a slight worsening in the *R* factor.

Structure solution and refinement to this stage were carried out on an Eclipse S140 computer using the SHELXTL program system.[34] Refinement was by block-cascade full-matrix least-squares to *R* = 0.14 for the non-hydrogen atoms. Because of program capacity limitations, the hydrogen atoms could not be allowed for using the above configuration. Further refinement was carried out with all the hydrogen positions, with the exception of those of the methanol molecules, idealised (C–H = 0.96 Å), assigned isotropic thermal parameters, U(H) = $1.2U_{eq}$(C), and allowed to ride on their parent carbons. Refinement was by blocked full-matrix least-squares to *R* = 0.13, $R_w = 0.12$ [w^{-1} = σ^2(*F*) + 0.0007F^2]. These subsequent calculations were carried out on the ULCC CRAY-1S computer using the SHELX-76 program system.

The fractional co-ordinates of the hydrogen atoms and isotropic thermal parameters and the anisotropic thermal parameters for the non-hydrogen atoms, have been deposited as Supplementary Data, No. SUP 56173 (6 pp.), and the tables of structure factors are available from the editorial office on request.

Determination of Association Constants.—All u.v. spectra were measured on a Pye Unicam SP500 Series 2 ultraviolet–visible spectrophotometer at 25.5 °C. Measurements were carried out in both acetonitrile and acetone. Acetonitrile was distilled from phosphorus pentaoxide and acetone from potassium permanganate and then calcium chloride before use. The molar absorptivity, ε_D, for diquat bis(hexafluorophosphate) (2) was determined as 18.0 in acetonitrile and as 20.8 in acetone.

The experimental method will be illustrated for the complexation between diquat bis(hexafluorophosphate) (2) and DB30C10 (14) in acetonitrile. A standard solution containing equimolar amounts of (2) and (14) in acetonitrile was made up in a 5 ml calibrated flask, and the solution's absorbance at 400 nm, A, was recorded. The solution was diluted accurately, and the new solution's absorbance, A, was measured. The process of accurate dilution and remeasurement of absorbance was repeated several times. In total, seven sets of data (concentration, d, absorbance, A) were obtained and the derived data points $[d/A_C, 1/(A_C)^{\frac{1}{2}}]$ were calculated as described earlier.

For the series of solutions described above, accurate dilution factors, and thence concentrations, d, were determined gravimetrically. However, each of the solutions was made up in the same 5 ml calibrated flask. That there was no correlation between (*i*) the concentration of the series of solutions, which contained progressively smaller amounts of solute and, (*ii*) the weight of the 5 ml portions of those solutions, confirmed our belief that the errors introduced by the adoption of gravimetric dilution were small compared with other experimental errors.

The experiment was repeated with a second standard solution, and seven-fold dilution yielded a set of eight data points. The two sets of points were judged to belong to the same population and were treated as one set of 15 points in the manner described below.

Association constants, K_a, and derived free energies of complexation, $\Delta G°$, for 1:1 complex formation in acetonitrile or acetone at 25.5 °C between diquat bis(hexafluorophosphate) (2) and the molecular receptors, DB27C9 (13), DB30C10 (14), DB33C11 (15), DB36C12 (16), and DN30C10 (27), are summarised in Table 6. In each experiment the linear relationship (*q.v.*. Figure 8) between d/A_C and $1/(A_C)^{\frac{1}{2}}$ was demonstrated by calculation of the sample correlation coefficient (see Table 6). In all cases, the correlation coefficient was >0.99. The two regression lines were calculated by the method of least squares. For each regression line, a value for the association constant, K_a, was obtained from the appropriate relationship between K_a and the slope (*m*) and intercept (*b*) of the line. For regression of d/A_C on $1/(A_C)^{\frac{1}{2}}$, $K_a = b/m^2$. For regression of $1/(A_C)^{\frac{1}{2}}$ on d/A_C, $K_a = -bm$. Additionally, an estimate of the error in K_a was obtained from the standard errors in m and b. The two values of K_a were averaged to give a value (which is that quoted in Table 6) from which a standard free energy of complexation, $\Delta G°$, was calculated; the value of K_a obtained by this method differed only slightly ($<1\%$ difference) from that value of K_a calculated from the line which (*i*) passes through the intersection of the two regression lines, and (*ii*) bisects the angle between them.

The acquisition and analysis of the data for the 2:1 (guest:host) complexation between diquat bis(hexafluorophosphate) (2) and DB24C8 (11) in acetone followed the same pattern as described above for the complexes with 1:1 stoicheiometry.

Acknowledgements

References

1 H. M. Colquhoun, J. F. Stoddart, D. J. Williams, J. B. Wolstenholme, and R. Zarzycki, *Angew. Chem., Int. Ed. Engl.*, 1981, **20**, 1051.
2 H. M. Colquhoun, S. M. Doughty, J. M. Maud, J. F. Stoddart, D. J. Williams, and J. B. Wolstenholme, *Isr. J. Chem.*, in the press.
3 C. J. Pedersen, *J. Am. Chem. Soc.*, 1967, **89**, 7017.
4 L. A. Summers, 'The Bipyridinium Herbicides,' Academic Press, London, 1980.
5 H. M. Colquhoun, E. P. Goodings, J. M. Maud, J. F. Stoddart, D. J. Williams, and J. B. Wolstenholme, *J. Chem. Soc., Chem. Commun.*, 1983, 1140.
6 J. Dale and P. O. Kristiansen, *Acta Chem. Scand.*, 1972, **26**, 1471.
7 R. M. Izatt, R. E. Terry, D. P. Nelson, Y. Chan, D. J. Eatough, J. S. Bradshaw, L. D. Hansen, and J. J. Christensen, *J. Am. Chem. Soc.*, 1976, **98**, 7626.
8 J. Druey, *Bull. Soc. Chim. Fr.*, 1935, 1737.
9 R. F. Homer and T. E. Tomlinson, *J. Chem. Soc.*, 1960, 2498; R. F. Homer, G. C. Mees, and T. E. Tomlinson, *J. Sci. Food Agric.*, 1960, **11**, 309.
10 I. C. Calder, T. M. Spotswood, and C. I. Tanzer, *Aust. J. Chem.*, 1967, **20**, 1195.
11 R. Hague, W. R. Coshow, and L. F. Johnson, *J. Am. Chem. Soc.*, 1969, **91**, 3822; R. Hague and S. Lilley, *J. Agric. Food Chem.*, 1972, **20**, 57.
12 T. Sundaresan and S. C. Wallwork, *Acta Crystallogr.*, 1972, **28B**, 3065.
13 N. Roh and B. Emmert, *Chem. Ber.*, 1925, **58B**, 503; B. Emmert, O. Schneider, and M. Koberne, *ibid.*, 1931, **64B**, 950; A. Ledwith and D. H. Iles, *Chem. Br.*, 1968, **4**, 266; A. Ledwith and H. J. Woods, *J. Chem. Soc. C*, 1970, 1422.
14 K. W. Ratts, R. K. Howe, and W. G. Phillips, *J. Am. Chem. Soc.*, 1969, **91**, 6115.
15 R. Foster and C. A. Fyfe, *Prog. Nucl. Magn. Reson. Spectrosc.*, 1969, **4**, 1.
16 B. G. White, *Trans. Faraday Soc.*, 1969, **65**, 2000.
17 J. E. Derry and T. A. Hamor, *Nature*, 1969, **221**, 464; P. D. Sullivan and M. L. Williams, *J. Am. Chem. Soc.*, 1976, **98**, 1711.
18 O. Hofer, *Monatsh. Chem.*, 1978, **109**, 405.
19 G. M. Anderson III, P. A. Kollman, L. N. Dommelsmith, and K. N. Houk, *J. Am. Chem. Soc.*, 1979, **101**, 2344; L. N. Dommelsmith, T. A. Eaton, N. K. Houk, G. M. Anderson III, R. A. Glennon, A. T. Shulgin, N. Castagnoli, Jr., and P. A. Kollman, *J. Med. Chem.*, 1981, **24**, 1414; A. Makriyannis and S. Fesik, *J. Am. Chem. Soc.*, 1982, **104**, 6462; L. I. Kruse and J. K. Cha, *J. Chem. Soc., Chem. Commun.*, 1982, 1329; J. D. Mersh, J. K. M. Sanders, and S. A. Matlin, *ibid.* 1983, 306.
20 M. A. Bush and M. R. Truter, *J. Chem. Soc., Perkin Trans. 2*, 1972, 345.
21 R. Foster, 'Organic Charge-Transfer Complexes,' Academic Press, London, 1969, p. 216.
22 T. T. Harding and S. C. Wallwork, *Acta Crystallogr.*, 1953, **6**, 791; G. G. Shipley and S. C. Wallwork, *ibid.*, 1967, **22**, 585, 593.
23 Ref. 21, p. 113.
24 R. J. Abraham and P. Loftus, 'Proton and Carbon-13 NMR Spectroscopy,' Heyden, London, 1978.
25 L. M. Jackman and S. Sternhell, 'Applications of Nuclear Magnetic Resonance Spectroscopy in Organic Chemistry,' Pergamon Press, Oxford, 1969, 2nd edn.
26 D. Live and S. I. Chan, *J. Am. Chem. Soc.*, 1976, **98**, 3769.
27 Ref. 21, p. 125.
28 Ref. 21, p. 179.
29 A. Ray, *J. Am. Chem. Soc.*, 1971, **93**, 7146.
30 G. W. Gokel, D. J. Cram, C. L. Liotta, H. P. Harris, and F. L. Cook, *J. Org. Chem.*, 1974, **39**, 2445; A. El Basynony, J. Klimes, A. Knöchel, J. Dehler, and G. Z. Rudolph, *Z. Naturforsch.*, 1976, **31B**, 1192; H. M. Colquhoun, J. F. Stoddart, and D. J. Williams, *J. Am. Chem. Soc.*, 1982, **104**, 1426; B. L. Allwood, S. E. Fuller, P. C. Y. K. Ning, A. M. Z. Slawin, J. F. Stoddart, and D. J. Williams, *J. Chem. Soc., Chem. Commun.*, 1984, 1356; J. F. Stoddart, S. E. Fuller, S. M. Doughty,

P. C. Y. K. Ning, M. K. Williams, D. J. Williams, B. L. Allwood, A. M. Z. Slawin, and H. M. Colquhoun, *Pure Appl. Chem.*, in the press.
31 W. C. Still, M. Kahn, and A. Mitra, *J. Org. Chem.*, 1978, **43**, 2923.
32 C. M. Elliott and E. J. Hershenhart, *J. Am. Chem. Soc.*, 1982, **104**, 7519.
33 W. D. Curtis, D. A. Laidler, J. F. Stoddart, and G. H. Jones, *J. Chem. Soc., Perkin Trans. 1*, 1977, 1756.

34 G. M. Sheldrick, SHELXTL, An Integrated System for Solving, Refining, and Displaying Crystal Structures from Diffraction Data, University of Göttingen, Federal Republic of Germany, 1978.